ARTICLE

LMI-based design of state-feedback controllers for pole clustering of LPV systems in a union of $\mathcal{D}_R$-regions

Ruicong Yang[a], Damiano Rotondo[b] and Vicenç Puig[a,c]

[a]Institut de Robòtica i Informàtica Industrial, CSIC-UPC, Llorens i Artigas 4-6, 08028, Barcelona, Spain; [b]Department of Electrical Engineering and Computer Science (IDE), University of Stavanger, Kristine Bonnevies vei 22, 4021, Stavanger, Norway; [c]Department of Automatic Control (ESAII), Technical University of Catalonia (UPC), Rambla de Sant Nebridi 10, 08222 - Terrassa, Spain

ARTICLE HISTORY
Compiled October 12, 2021

ABSTRACT
This paper introduces an approach for the design of a state-feedback controller that achieves pole clustering in a union of $\mathcal{D}_R$-regions for linear parameter varying systems. The design conditions, obtained using a partial pole placement theorem, are eventually expressed in terms of linear matrix inequalities. In addition, it is shown that the approach can be modified in a shifting sense. Hence, the controller gain is computed such that different values of the varying parameters imply different regions of the complex plane where the closed-loop poles are situated. This approach enables the online modification of the closed-loop performance. The effectiveness of the proposed method is demonstrated by means of simulations.

KEYWORDS
Linear parameter varying (LPV) systems, pole placement, union of regions, linear matrix inequalities (LMIs), state-feedback control.

1. Introduction

Linear parameter varying (LPV) systems have received a lot of attention from the control community in the last decades. They were first introduced by Shamma (1988), in order to distinguish such systems from linear time invariant (LTI) and linear time varying (LTV) (Shamma, 2012). The LPV paradigm has proved to be suitable for controlling nonlinear systems by embedding the nonlinearities in the varying parameters, and it has become a standard formalism in systems and control, for analysis, synthesis of controllers and even system identification. In this case, since the varying parameters depend on some endogenous signals, such as states and/or inputs, the system is commonly referred to as quasi-LPV (Rugh & Shamma, 2000). LPV systems are closely related to the Takagi-Sugeno (TS) approach (Li & Yang, 2019; Takagi & Sugeno, 1985; L. Zhang, Jia, & Yang, 2020), and some recent works have discussed the existing similarities between the two approaches (López-Estrada, Rotondo, & Valencia-Palomo, 2019; Rotondo, Puig, & Nejjari, 2016; Rotondo, Puig, Nejjari, & Witczak, 2015). In particular, Rotondo, Puig, et al. (2015) stated that the main remarkable difference be-

CONTACT Ruicong Yang. Email: ruicong.yang@upc.edu

tween the two frameworks is the set of mathematical tools that are used for obtaining the system description. In the LPV case, these tools belong to the standard mathematics; on the other hand, in the TS case, they belong to the fuzzy theory. More recently, there has been a growing interest in extending these techniques to nonlinear parameter varying systems (NLPV), see e.g. Larimore (2013), Blesa, Jiménez, Rotondo, Nejjari, and Puig (2014), Rotondo and Johansen (2018), R. Yang, Rotondo, and Puig (2019), since in many practical applications there are time-varying nonlinearities that can be dealt with using ad hoc approaches.

In recent years, there has been an important progress in the development of analysis and design techniques for LPV system, and this concept has been further investigated by several researchers, who brought different innovations (Hoffmann & Werner, 2014; Rotondo, 2017). LPV techniques have found application in many fields, such as riderless bicycles (Brizuela Mendoza, Sorcia Vázquez, Guzmán Valdivia, Osorio Sánchez, & Martínez García, 2018), robotics (San Miguel, Puig, & Alenyà, 2019), aerospace (D. Yang, Zong, & Karimi, 2019), ground vehicles (H. Zhang, Zhang, & Wang, 2016), wind turbines (Pérez-Estrada, Osorio-Gordillo, Alma, Darouach, & Olivares-Peregrino, 2018) and power systems (El-Guindy, Schaab, Schürmann, Stursberg, & Althoff, 2017). Remarkable applications can be mentioned as machine learning (Rizvi, Velni, Abbasi, Tóth, & Meskin, 2018), and model predictive control (MPC) (Ding, Dong, & Hu, 2019), and the research is currently undergoing theoretical development (Morato, Normey-Rico, & Sename, 2020).

Among the considered specifications for the design, placing poles in linear matrix inequality (LMI) regions, also known as $\mathcal{D}$-stability, has received a lot of interest. Initially characterized by Chilali and Gahinet (1996) using a quadratic Lyapunov function with constant matrix, this idea was further developed by Peaucelle, Arzelier, Bachelier, and Bernussou (2000), who considered uncertain systems by means of a parameter dependent Lyapunov function, and is still investigated nowadays, see e.g. the recent improvements in Nguyen, Márquez, Guerra, and Dequidt (2017) and Chesi (2017). However, LMI regions have some limitations, such that they are not able of describing non-convex regions or the union of different regions. For this reason, Peaucelle et al. (2000) proposed a new characterization of LMI regions referred to as $\mathcal{D}_R$-regions and considered uncertain systems by means of a parameter-dependent Lyapunov function. In Peaucelle et al. (2000), $\mathcal{D}_R$-regions were shown to be able to describe non-convex regions but only represented symmetrically, which motivated Bosche, Bachelier, and Mehdi (2005) to extend the concept further to consider non-symmetrical regions. On the other hand, Bachelier and Pradin (1999) developed an approach that allows specifying not only simple convex regions, but also non-convex regions, defined as the unions of convex subregions. Then, Maamri, Bachelier, and Mehdi (2006) proposed a technique in order to achieve partial pole placement via aggregation in such regions. It was demonstrated that this method can influence strongly the performance, in terms of settling time and damping ratio. In Tornil-Sin, Theilliol, Ponsart, and Puig (2010), this method was applied to fault-tolerant control.

Although the concept of *pole* is not formally defined for LPV systems, Ghersin and Sanchez-Peña (2002) showed that by including pole clustering specifications in the LPV design, the performance of the LPV control systems could be improved. Moreover, R. Yang et al. (2019) showed the existence of a relationship between pole clustering and the Lyapunov function. In fact, pole placement for gain-scheduled systems has progressed strongly in the last decades, with several results concerning the design of observers (Nejjari, Puig, de Oca, & Sadeghzadeh, 2009), state-feedback controllers (Bouazizi, Kochbati, & Ksouri, 2001; R. Yang et al., 2019), H_∞ controllers (Rotondo,

Nejjari, & Puig, 2014; Yu, Chen, & Woo, 2002), PID controllers (Rabaoui, Hamdi, Braiek, & Rodrigues, 2020) and applications in many fields, such as aerospace vehicles (Ghersin & Sanchez-Peña, 2002), UAVs (López-Estrada, Ponsart, Theilliol, Zhang, & Astorga-Zaragoza, 2016), aircrafts (Zhenxing & Jun, 2019), mechanical cranes (López-Estrada, Santos-Estudillo, Valencia-Palomo, Gómez-Peñate, & Hernandez-Gutiérrez, 2020), missiles (Shen, Yu, Luo, & Mei, 2017), power systems (Jabali & Kazemi, 2017a), fuel cells (Rotondo, Fernandez-Canti, Tornil-Sin, Blesa, & Puig, 2016) and robotics (Jabali & Kazemi, 2017b).

In fact, *pole placement* and *pole clustering* have been used in the literature as synonyms to denote moving poles to the same region of the complex plane, whereas in this paper we denote as *pole clustering* the process of moving them to different regions and as *pole placement* the process of moving them to a single common region for all the poles. On the other hand, based on the literature review, it seems that the aforementioned partial pole clustering technique has not been applied yet to gain-scheduled systems, such as LPV and TS. The present work is the first one to consider partial pole clustering for such systems. Such an extension is not trivial, as the design of controller gains through aggregation introduces nonlinearities that destroy the polytopic decomposition usually exploited in the LPV controller design. The advantage of the proposed control design approach is that the performance can be fine-tuned by choosing multiple desired regions where the poles are placed. Unlike the traditional pole placement, pole clustering can move the system's poles into different regions, so that the designer has much more control over the closed-loop performance that can be achieved.

Motivated by this fact, the main goal of this paper is to consider the problem of designing an LPV state-feedback controller for LPV systems that can guarantee some desired closed-loop poles clustering in a region defined as the union of disjoint subregions. It is shown that it is possible to exploit the aggregation technique initially proposed for LTI systems by Maamri et al. (2006) to achieve partial pole placement in LPV systems, so that disjoint regions can be assigned for the closed-loop distribution of the poles. The proposed design conditions are formulated through an LMI approach. In order to deal with the nonlinearities introduced by the eigendecomposition required to achieve partial pole placement, new varying parameters are introduced so that a polytopic representation can be recovered.

In addition to the classical pole clustering problem, in this paper, we consider also an extension referred to as *shifting pole placement* (Rotondo, Nejjari, & Puig, 2013, 2015). This approach allows designing the controller gain in such a way that different values of the varying parameters imply different regions where the closed-loop poles are situated. By means of the shifting paradigm, the online modification of the performance can be achieved, as demonstrated for example by Ruiz, Rotondo, and Morcego (2019) and Ruiz, Rotondo, and Morcego (2020), who have applied this concept to saturated system showing that it is possible to schedule the closed-loop performance according to changes in the saturation function.

The main contributions of this paper can be summarized as follows:

- The partial pole placement originally developed in Maamri et al. (2006) for LTI systems is extended to work with LPV systems.
- A procedure for the design of a state-feedback controller which achieves pole clustering in a union of $\mathcal{D}_R$-regions is proposed for LPV systems.
- It is shown that in spite of the nonlinearities introduced by the aggregation technique, it is possible to introduce new sets of varying parameters in terms of

which polytopic representations suitable for reducing the number of design LMIs from infinite to finite can be obtained.

The rest of the paper is organized as follows. In Section 2, partial pole placement background information is introduced. Section 3 explains in detail the pole clustering in a union of regions for LPV systems. Section 4 discusses how the approach can be extended according to the shifting paradigm. Section 5 shows the application of the developed technique to a numerical example and a two-tank system. Finally, Section 6 summarizes the conclusions and suggests possible future work.

Notation: $\mathbb{R}^{n\times m}$ and $\mathbb{C}^{n\times m}$ denote the set of real and complex matrices with n rows and m columns; A^T, A^* and A^+ denote the transpose, the conjugate and the pseudo-inverse of A, respectively; A^H is the Hermitian matrix defined as $A^H = A + A^*$; the Euclidean norm is indicated by $||A||$; $\otimes$ represents the Kronecker product; in matrix inequalities, negative (semi-)definiteness is indicated by $\prec 0$ ($\preceq 0$), whereas $\succ 0$ ($\succeq 0$) denotes positive (semi-)definiteness.

2. Background

The idea of LMI regions was first introduced by Chilali and Gahinet (1996) in order to provide a Lyapunov-based characterization of pole clustering in stable subregions of the complex plane. Their formal definition is given as follows:

Definition 1: *(LMI region)* (Chilali & Gahinet, 1996) A subset $\mathcal{D}$ of the complex plane is called an LMI region if there exist a matrix $\alpha = [\alpha_{kl}] \in \mathbb{S}^{m\times m}$ and a matrix $\beta = [\beta_{kl}] \in \mathbb{R}^{m\times m}$ such that:

$$\mathcal{D} = \{s \in \mathbb{C} : f_{\mathcal{D}} \prec 0\} \tag{1}$$

with the *characteristic function* given by:

$$f_{\mathcal{D}}(s) = \alpha + s\beta + s^*\beta^T = [\alpha_{kl} + \beta_{kl}s + \beta_{lk}s^*]_{1\leq k,l\leq m}\,. \tag{2}$$

In other words, LMI regions are subsets of the complex plane that are represented by an LMI in s and s^*. In addition, a new characterization of regions was proposed in Peaucelle et al. (2000) called $\mathcal{D}_R$-regions.

Definition 2: *($\mathcal{D}_R$-regions)* (Peaucelle et al., 2000) Let R be a $2d \times 2d$ Hermitian matrix defined as:

$$R = \begin{bmatrix} R_{00} & R_{10} \\ R_{10}^* & R_{11} \end{bmatrix} \in \mathbb{C}^{2d\times 2d}. \tag{3}$$

Then, the subset of the complex plane defined according to

$$\mathcal{D}_R = \{s \in \mathbb{C} : R_{00} + (R_{10}s)^H + R_{11}s^*s \prec 0\} \tag{4}$$

is called a $\mathcal{D}_R$-region of degree d.

The class of $\mathcal{D}_R$-regions is a class of open convex subsets of the complex plane that includes (among others) half-planes, disks, conic sectors, vertical and horizontal strips

and ellipses, symmetrical or not with respect to the real axis. For example, the vertical left half-plane defined by $Re(s) < \lambda$ is characterized by a matrix R equal to:

$$R = \begin{bmatrix} -2\lambda & 1 \\ 1 & 0 \end{bmatrix}, \tag{5}$$

while the interior of a disk with center $c = c_1 + c_2 i$ and radius r is characterized by:

$$R = \begin{bmatrix} c_1^2 + c_2^2 - r^2 & -c_1 + c_2 i \\ -c_1 - c_2 i & 1 \end{bmatrix}. \tag{6}$$

In contrast to LMI regions, $\mathcal{D}_R$-regions are able to represent non-convex regions. Without any assumption on the matrix R_{11}, $\mathcal{D}_R$-regions are not convex, but with $R_{11} \succ 0$, $\mathcal{D}_R$-regions become a slight modification of the characterization provided by LMI regions (Rotondo, 2017). In Bachelier and Pradin (1999), non-convex regions were considered as unions of convex subregions.

Before introducing the partial pole placement for LPV systems, let us recall the existing approach for LTI system (Maamri et al., 2006).

Let us consider the following system:

$$\dot{x}(t) = Ax(t) + Bu(t). \tag{7}$$

Then, the following lemmas can be applied:

Lemma 1 (Peaucelle et al., 2000): *The matrix A is said to be $\mathcal{D}_R$-stable, or in other words all its eigenvalues lie inside the region $\mathcal{D}_R$ if and only if there exists a matrix $P \succ 0$ such that:*

$$R_{00} \otimes P + (R_{10} \otimes (PA))^H + R_{11} \otimes (A^* P A) \prec 0. \tag{8}$$

In Maamri et al. (2006), Lemma 1 has been extended to partial pole placement in $\mathcal{D}_R$, which means that only p eigenvalues are wished to be affected by the feedback. To do so, some matrices are defined as follows:

$$\Lambda = V^{-1} A V = \begin{bmatrix} \Lambda_1 & 0 \\ 0 & \Lambda_2 \end{bmatrix}, \quad G = \begin{bmatrix} I_p & 0 \end{bmatrix} V^{-1},$$
$$G^+ = V \begin{bmatrix} I_p \\ 0 \end{bmatrix}, \quad \hat{A} = GAG^+ \quad \text{and} \quad \hat{B} = GB,$$

where V is the modal matrix of A, that is, the matrix whose columns are the (possibly generalized) eigenvectors of A. $\Lambda_1 \in \mathbb{C}^{p \times p}$ is associated to the set of p eigenvalues desired to be affected by the feedback, whereas Λ_2 denotes the remaining eigenvalues.

Then, the following lemma can be applied:

Lemma 2 (Maamri et al., 2006): *There exists a state-feedback gain $\hat{K}$ that assigns p poles in $\mathcal{D}_R$ if and only if there exist an matrix $\hat{X} \succ 0$ and a matrix $\hat{S}$ such that the LMI:*

$$\begin{bmatrix} R_{00} \otimes \hat{X} + (R_{10} \otimes (\hat{A}\hat{X} + \hat{B}\hat{S}))^H & Z^* \otimes (\hat{A}\hat{X} + \hat{B}\hat{S})^* \\ Z \otimes (\hat{A}\hat{X} + \hat{B}\hat{S}) & -I_d \otimes \hat{X} \end{bmatrix} \prec 0 \tag{9}$$

holds, where Z is deduced from the Cholesky factorization $R_{11} = Z^*Z$. In this case, a suitable state-feedback gain is:

$$\hat{K} = \hat{S}\hat{X}^{-1}. \tag{10}$$

3. Pole clustering in a union of regions for LPV system

In this section, the aggregation technique is extended to LPV systems to compute a state-feedback controller gain which performs pole clustering in a union of regions for LPV systems.

Let us recall that an LPV system is defined as a finite-dimensional time-varying system whose state equation, although linear, is described by matrices which are function of some varying parameters $\theta(t) \in \Theta \subset \mathbb{R}^{n_\theta}$ (with Θ known closed set), that are assumed to be unknown a priori, but that can be measured or estimated in real-time:

$$\dot{x}(t) = A(\theta(t))x(t) + B(\theta(t))u(t), \tag{11}$$

where $A(\theta(t)) \in \mathbb{R}^{n_x \times n_x}$, $B(\theta(t)) \in \mathbb{R}^{n_x \times n_u}$ are the state and input matrices, $x(t) \in \mathbb{R}^{n_x}$ denotes the system state, $u(t) \in \mathbb{R}^{n_u}$ is the control input. The system (11) is said to be polytopic if it can be represented by state-space matrices $A(\theta(t))$ and $B(\theta(t))$ which range over a convex set:

$$\dot{x}(t) = \sum_{n=1}^{w} \mu_n(\theta(t))\big(A_n x(t) + B_n u(t)\big), \tag{12}$$

where μ_n are the non-negative coefficients of the polytopic decomposition such that:

$$\sum_{n=1}^{w} \mu_n(\theta(t)) = 1, \quad \mu_n(\theta(t)) \geq 0, \quad \forall n = 1, ..., w \quad \text{and} \quad \forall \theta \in \Theta.$$

Let us use a gain-scheduled state-feedback control law given by:

$$u(t) = K(\theta(t))x(t), \tag{13}$$

where $K(\theta(t))$ is the controller gain to be designed.

3.1. Aggregation technique

The main idea of the algorithm employed to achieve pole clustering in a union of regions is to use a structured feedback gain $K(\theta(t))$ that modifies just a subset of the system poles. The following equations are the "preconditions" for the partial pole-clustering. Consider the Jordan canonical form for the matrix $A(\theta(t))$:

$$\Lambda(\theta(t)) = V(\theta(t))^{-1} A(\theta(t)) V(\theta(t)), \tag{14}$$

where $V(\theta(t))$ is the modal matrix of $A(\theta(t))$, which means that the columns of $V(\theta(t))$ are the (possibly generalized) eigenvectors of $A(\theta(t))$.

On the other hand, $\Lambda(\theta(t))$ can be rearranged in a form such that:

$$\Lambda(\theta(t)) = \begin{bmatrix} \Lambda_1(\theta(t)) & 0 \\ 0 & \Lambda_2(\theta(t)) \end{bmatrix}, \tag{15}$$

where the transformation is used to obtain the matrix $\Lambda_1(\theta(t)) \in \mathbb{C}^{p\times p}$ which contains the p eigenvalues that are wished to be affected by the feedback using the partial pole placement algorithm. Let us define the following matrices:

$$G(\theta(t)) = \begin{bmatrix} I_p & 0 \end{bmatrix} V(\theta(t))^{-1}, \tag{16}$$

with pseudo-inverse given by:

$$G(\theta(t))^{+} = V(\theta(t)) \begin{bmatrix} I_p \\ 0 \end{bmatrix} \tag{17}$$

are used for extracting the part of the eigenvectors that associated to the set of p eigenvalues, and similar as:

$$\hat{A}(\theta(t)) = G(\theta(t))A(\theta(t))G(\theta(t))^{+}, \tag{18}$$

$$\hat{B}(\theta(t)) = \begin{bmatrix} I_p & 0 \end{bmatrix} V(\theta(t))^{-1}B(\theta(t)), \tag{19}$$

$$\bar{B}(\theta(t)) = \begin{bmatrix} 0 & I_{n-p} \end{bmatrix} V(\theta(t))^{-1}B(\theta(t)) \tag{20}$$

are used to select the parts of the system that are associated to the set of p eigenvalues that will be moved during the iteration of the algorithm, and finally, consider a feedback gain defined as:

$$K(\theta(t)) = \hat{K}(\theta(t))G(\theta(t)). \tag{21}$$

The closed-loop matrix then satisfies:

$$\begin{aligned}
&A(\theta(t)) + B(\theta(t))K(\theta(t)) = A(\theta(t)) + B(\theta(t))\hat{K}(\theta(t))G(\theta(t)) \\
&= A(\theta(t)) + B(\theta(t))\hat{K}(\theta(t)) \begin{bmatrix} I_p & 0 \end{bmatrix} V(\theta(t))^{-1} \\
&= V(\theta(t))\Big(V(\theta(t))^{-1}A(\theta(t))V(\theta(t)) + V(\theta(t))^{-1}B(\theta(t))\hat{K}(\theta(t)) \begin{bmatrix} I_p & 0 \end{bmatrix}\Big)V(\theta(t))^{-1} \\
&= V(\theta(t))\Big(\begin{bmatrix} \Lambda_1(\theta(t)) & 0 \\ 0 & \Lambda_2(\theta(t)) \end{bmatrix} + \begin{bmatrix} I_p & 0 \\ 0 & I_{n-p} \end{bmatrix} V(\theta(t))^{-1}B(\theta(t))\hat{K}(\theta(t)) \begin{bmatrix} I_p & 0 \end{bmatrix}\Big)V(\theta(t))^{-1} \\
&= V(\theta(t))\Big(\begin{bmatrix} \Lambda_1(\theta(t)) & 0 \\ 0 & \Lambda_2(\theta(t)) \end{bmatrix} + \begin{bmatrix} \hat{B}(\theta(t))\hat{K}(\theta(t)) & 0 \\ \bar{B}(\theta(t))\hat{K}(\theta(t)) & 0 \end{bmatrix}\Big)V(\theta(t))^{-1} \\
&= V(\theta(t)) \begin{bmatrix} \Lambda_1(\theta(t)) + \hat{B}(\theta(t))\hat{K}(\theta(t)) & 0 \\ \bar{B}(\theta(t))\hat{K}(\theta(t)) & \Lambda_2(\theta(t)) \end{bmatrix} V(\theta(t))^{-1}
\end{aligned} \tag{22}$$

which means that the eigenvalues associated to $\Lambda_1(\theta(t))$ are modified whereas the eigenvalues of $\Lambda_2(\theta(t))$ are invariant with respect to the feedback $K(\theta(t)) =$

$\hat{K}(\theta(t))G(\theta(t))$, i.e. such feedback gain will only modify the p eigenvalues of interest.

3.2. Partial $\mathcal{D}_R$-stability

In order to extend the pole clustering in a union of regions to LPV system, let us consider the $\mathcal{D}_R$-stability of the LPV system (11), in the sense of all the frozen poles of (11) lying in $\mathcal{D}_R$. By applying Lemma 1, $\mathcal{D}_R$-stability holds if there exists a matrix $P \succ 0$ such that $\forall\theta \in \Theta$:

$$R_{00} \otimes P + (R_{10} \otimes (PA(\theta(t))))^H + R_{11} \otimes (A(\theta(t))^* PA(\theta(t))) \prec 0. \tag{23}$$

The above means that for partial pole placement in $\mathcal{D}_R$ being achieved by the state-feedback gain $\hat{K}(\theta(t))$, the gain has to be chosen in such a way that it satisfies:

$$\begin{aligned} &R_{00} \otimes \hat{P} + (R_{10} \otimes (\hat{P}(\hat{A}(\theta(t)) + \hat{B}(\theta(t))\hat{K}(\theta(t)))))^H + ... \\ &... + R_{11} \otimes ((\hat{A}(\theta(t)) + \hat{B}(\theta(t))\hat{K}(\theta(t)))^* \hat{P}(\hat{A}(\theta(t)) + \hat{B}(\theta(t))\hat{K}(\theta(t)))) \prec 0 \end{aligned} \tag{24}$$

for some matrix $\hat{P} \succ 0$.

Deduced from the above, the next theorem states LMI conditions for obtaining a controller gain that achieve partial pole placement.

Theorem 1: There exists a state-feedback gain $\hat{K}(\theta)$ that assigns p eigenvalues of the closed-loop matrix $A(\theta) + B(\theta)\hat{K}(\theta)G(\theta)$ in the region $\mathcal{D}_R$ defined by (4) if there exist matrices $\hat{X} \succ 0$ and $\hat{S}(\theta)$ of appropriate dimensions such that $\forall\theta \in \Theta$:

$$\begin{bmatrix} R_{00} \otimes \hat{X} + (R_{10} \otimes (\hat{A}(\theta)\hat{X} + \hat{B}(\theta)\hat{S}(\theta)))^H & Z^* \otimes (\hat{A}(\theta)\hat{X} + \hat{B}(\theta)\hat{S}(\theta))^* \\ Z \otimes (\hat{A}(\theta)\hat{X} + \hat{B}(\theta)\hat{S}(\theta)) & -I_d \otimes \hat{X} \end{bmatrix} \prec 0, \tag{25}$$

where Z is deduced from the Cholesky factorization $R_{11} = Z^*Z$. Then, the state-feedback gain is given by:

$$\hat{K}(\theta(t)) = \hat{S}(\theta(t))\hat{X}^{-1}. \tag{26}$$

Proof: It can be derived by following the steps in the proof of Theorem 2.1 in Maamri et al. (2006). □

Hence, the partial pole placement procedure boils down in obtaining a solution for the LMI (25), and then using (26) to recover the appropriate $\hat{K}(\theta(t))$.

It is necessary to mention that the design condition (25) requires satisfying an infinite number of conditions, which leads to a computational issue. In order to reduce the number of conditions from infinite to finite, the most common way to solve this problem is to use the polytopic assumption. However, the non-linearity introduced by the multiplications in (18) implies that even if a polytopic representation is available for $A(\theta(t))$, it does not necessarily hold that the same polytopic coefficients describe how $\hat{A}(\theta(t))$ varies with respect to $\theta(t)$. However, it is possible to introduce new varying parameters, that are some nonlinear function of the original varying parameters, hereafter denoted by $\hat{\theta}(t)$, and then obtain a polytopic representation for the matrix $\hat{A}$ with coefficients that depend on $\hat{\theta}$. This can be done using available methods in the literature, such as the *bounding box* (Sun & Postlethwaite, 1998) the *singular value*

decomposition boxing (Baranyi, 2009) or identification approaches (Fujimori & Ljung, 2005).

Hence, the matrices $\hat{A}(\theta(t))$ and $\hat{B}(\theta(t))$ are expressed as polytopic combination of matrices $\hat{A}_i$ and $\hat{B}_i$ as follows:

$$\hat{A}(\theta(t)) = \hat{A}(\hat{\theta}(t)) = \sum_{i=1}^{r} \alpha_i(\hat{\theta}(t))\hat{A}_i, \tag{27}$$

$$\hat{B}(\theta(t)) = \hat{B}(\hat{\theta}(t)) = \sum_{i=1}^{r} \alpha_i(\hat{\theta}(t))\hat{B}_i, \tag{28}$$

where α_i are the non-negative coefficients of the polytopic decomposition such that:

$$\sum_{i=1}^{r} \alpha_i(\hat{\theta}(t)) = 1, \quad \alpha_i(\hat{\theta}(t)) \geq 0, \quad \forall i = 1, ..., r \quad \text{and} \quad \forall \hat{\theta} \in \hat{\Theta} \subset \mathbb{R}^{n_{\hat{\theta}}} \tag{29}$$

and the matrix function $\hat{S}(\theta(t))$ is constrained to satisfy:

$$\hat{S}(\theta(t)) = \hat{S}(\hat{\theta}(t)) = \sum_{i=1}^{r} \alpha_i(\hat{\theta}(t))\hat{S}_i. \tag{30}$$

Then, the approach proposed by Sala and Ariño (2007) to check the definiteness of double polytopic sums (as the ones arising from the terms $\hat{B}(\theta)\hat{S}(\theta)$ in (25)) can be applied by choosing a scalar $s \in \mathbb{N}$ and using the symbols $\mathbb{P}_s$ and $\mathbb{P}_s^+$ to denote the following sets:

$$\mathbb{P}_s = \left\{ \vec{p} = [\vec{p}_1, \ldots, \vec{p}_s]^T \in \mathbb{N}^s | 1 \leq \vec{p}_k \leq s \, \forall k = 1, \ldots, s \right\}, \tag{31}$$

$$\mathbb{P}_s^+ = \left\{ \vec{p} \in \mathbb{P}_s | \vec{p}_k \leq \vec{p}_{k+1}, k = 1, \ldots, s-1 \right\}, \tag{32}$$

whereas $\mathcal{P}(\vec{p}) \subset \mathbb{P}_s$ denotes the set of permutations, with possible repeated elements, of the multi-index $\vec{p}$, thus obtaining the following corollary.

Corollary 1: For any $s \in \mathbb{N}$, with $s \geq 2$, there exist a matrix $\hat{X} \succ 0$ and matrices $\hat{S}_1, \hat{S}_2, \ldots, \hat{S}_r$ such that:

$$\sum_{\vec{m} \in \mathcal{P}(\vec{p})} \begin{bmatrix} R_{00} \otimes \hat{X} + (R_{10} \otimes (\hat{A}_{\vec{m}_1}\hat{X} + \hat{B}_{\vec{m}_2}\hat{S}_{\vec{m}_1}))^H & Z^* \otimes (\hat{A}_{\vec{m}_1}\hat{X} + \hat{B}_{\vec{m}_2}\hat{S}_{\vec{m}_1})^* \\ Z \otimes (\hat{A}_{\vec{m}_1}\hat{X} + \hat{B}_{\vec{m}_2}\hat{S}_{\vec{m}_1}) & -I_d \otimes \hat{X} \end{bmatrix} \prec 0 \tag{33}$$

holds $\forall \vec{p} \in \mathbb{P}_s^+$, where Z is obtained from the Cholesky factorization $R_{11} = Z^*Z$, then the state-feedback gain given by (26), with $\hat{S}$ computed using (30), assigns p eigenvalues of the closed-loop matrix $A(\theta) + B(\theta)\hat{K}(\theta)C(\theta)$ in the region $\mathcal{D}_R$ defined by (4).

Proof: Taking into account the definition of $\hat{A}(\theta(t))$, $\hat{B}(\theta(t))$ and $\hat{S}(\theta(t))$ in (27)-(30), the parameter-dependent LMI (25) is equivalent to:

$$\sum_{i=1}^{r}\sum_{j=1}^{r}\alpha_i(\hat{\theta})\alpha_j(\hat{\theta})\begin{bmatrix} R_{00}\otimes\hat{X}+(R_{10}\otimes(\hat{A}_i\hat{X}+\hat{B}_j\hat{S}_i))^H & Z^*\otimes(\hat{A}_i\hat{X}+\hat{B}_j\hat{S}_i)^* \\ Z\otimes(\hat{A}_i\hat{X}+\hat{B}_j\hat{S}_i) & -I_d\otimes\hat{X}\end{bmatrix}\prec 0 \tag{34}$$

which corresponds to the problem of verifying the negativity of a double polytopic sum. By applying Polya's theorem on definite quadratic forms (Sala & Ariño, 2007), (33) is obtained. □

As discussed by Sala and Ariño (2007), the sufficient conditions obtained through the application of Polya's theorem become progressively less conservative when s increases, and actually exact, i.e. necessary and sufficient, for a finite value of s.

3.3. Pole clustering in a union of regions for LPV systems

Assume now that the region of interest $\mathcal{D}$ is obtained as follows:

$$\mathcal{D}=\bigcup_{k=1}^{q}\mathcal{D}_{R_k}, \tag{35}$$

where each subregion $\mathcal{D}_{R_k}$ is a $\mathcal{D}_R$-region defined in (4). Then, the pole clustering in the region $\mathcal{D}$ can be performed by successive partial pole clustering in the subregions $\mathcal{D}_{R_k}$, for $k=1,...,q$. This can be achieved according to the following algorithm.

Algorithm 1

- **Step 1:** Consider the state matrix of the LPV system (12) and:

$$A(\theta(t))=\sum_{n=1}^{w}\mu_n(\theta(t))A_n. \tag{36}$$

- **Step 2:** Let $k=0$ and $A_0(\theta(t))=A(\theta(t))$.
- **Step 3:** Let $k=k+1$.
- **Step 4:** Compute $V_{k-1}(\theta(t))$ and $\Lambda_{k-1}(\theta(t))$ such that $A_{k-1}(\theta(t))V_{k-1}(\theta(t))=V_{k-1}(\theta(t))\Lambda_{k-1}(\theta(t))$; rearrange $\Lambda_{k-1}(\theta(t))$ and $V_{k-1}(\theta(t))$ in the form:

$$\Lambda_{k-1}(\theta(t))=\begin{bmatrix}\Lambda^1_{k-1}(\theta(t)) & 0\\ 0 & \Lambda^2_{k-1}(\theta(t))\end{bmatrix},$$

  where $\Lambda^1_{k-1}(\theta(t))$ contains the p_k eigenvalues to be shifted to $\mathcal{D}_{R_k}$; then calculate $G_{k-1}(\theta(t))$ as:

$$G_{k-1}(\theta(t))=\begin{bmatrix}I_{p_k} & 0\end{bmatrix}V_{k-1}(\theta(t))^{-1}.$$

- **Step 5:** Compute:

$$\hat{A}_{k-1}(\theta(t))=G_{k-1}(\theta(t))A_{k-1}(\theta(t))G_{k-1}(\theta(t))^{+}, \tag{37}$$

$$\hat{B}_{k-1}(\theta(t))=G_{k-1}(\theta(t))B_{k-1}(\theta(t)). \tag{38}$$

- **Step 6:** Obtain a polytopic representation for $\hat{A}_{k-1}(\theta(t))$ and $\hat{B}_{k-1}(\theta(t))$ in terms of dependence on a new scheduling vector $\hat{\theta}_{k-1}$:

$$\hat{A}_{k-1}(\theta(t)) = \hat{A}_{k-1}(\hat{\theta}_{k-1}(t)) = \sum_{i=1}^{r} \alpha_{k-1,i}(\hat{\theta}_{k-1}(t))\hat{A}_{k-1,i}, \tag{39}$$

$$\hat{B}_{k-1}(\theta(t)) = \hat{B}_{k-1}(\hat{\theta}_{k-1}(t)) = \sum_{i=1}^{r} \gamma_{k-1,i}(\hat{\theta}_{k-1}(t))\hat{B}_{k-1,i}. \tag{40}$$

- **Step 7:** Find matrices $\hat{X}_k > 0$ and $\hat{S}_k(\hat{\theta}_{k-1}(t))$ such that Theorem 1/Corollary 1 holds, with $\hat{X} = \hat{X}_k$, $\hat{S}(\theta_{k-1}(t)) = \hat{S}_k(\hat{\theta}_{k-1}(t))$, $\hat{A}(\theta_{k-1}(t)) = \hat{A}_{k-1}(\hat{\theta}_{k-1}(t))$, $\hat{B}(\theta_{k-1}(t)) = \hat{B}_{k-1}(\hat{\theta}_{k-1}(t))$ and $R = R_k$. Then, calculate $\hat{K}_k(\hat{\theta}_{k-1}(t)) = \hat{S}_k(\hat{\theta}_{k-1}(t))\hat{X}_k^{-1}$.
- **Step 8:** Once $\hat{K}_k(\hat{\theta}_{k-1}(t))$ has been obtained, compute the state-feedback gain at step k as:

$$K_k(\theta(t), \hat{\theta}_{k-1}(t)) = \hat{K}_k(\hat{\theta}_{k-1}(t))G_{k-1}(\theta(t))$$

  and the closed-loop matrix at step k as:

$$A_k(\theta(t), \hat{\theta}_0(t), .., \hat{\theta}_{k-1}(t)) = A_{k-1}(\theta(t), \hat{\theta}_0(t), .., \hat{\theta}_{k-2}(t)) + B(\theta(t))K_k(\theta(t), \hat{\theta}_{k-1}(t)).$$

- **Step 9:** If $k \neq q$ then go to **Step 3**
- **Step 10:** The final state-feedback gain that achieves partial pole clustering in union of regions is given by:

$$K(\theta(t), \hat{\theta}_0(t), ..., \hat{\theta}_{q-1}(t)) = \sum_{k=1}^{q} K_k(\theta(t), \hat{\theta}_{k-1}(t)) \tag{41}$$

  that achieves the desired pole clustering in the specified union of regions.
- **Step 11:** Stop

Fig. 1 shows a graphical flowchart of the algorithm.
In order to do the online implementation, the algorithm is given as follows:
Algorithm 2

- **Step 1:** Consider the varying parameter $\vartheta(t)$ for state matrix of the LPV system (12) and

$$A(\vartheta(t)) = \sum_{n=1}^{w} \mu_n(\vartheta(t))A_n. \tag{42}$$

- **Step 2:** Let $k = 0$ and $A_0(\vartheta(t)) = A(\vartheta(t))$.
- **Step 3:** Let $k = k + 1$.
- **Step 4:** Compute the matrices $V_{k-1}(\vartheta(t))$, $\Lambda_{k-1}(\vartheta(t))$, $G_{k-1}(\vartheta(t))$, $\hat{A}_{k-1}(\vartheta(t))$ and $\hat{B}_{k-1}(\vartheta(t))$ same as in Step 4 and 5 in Algorithm 1.

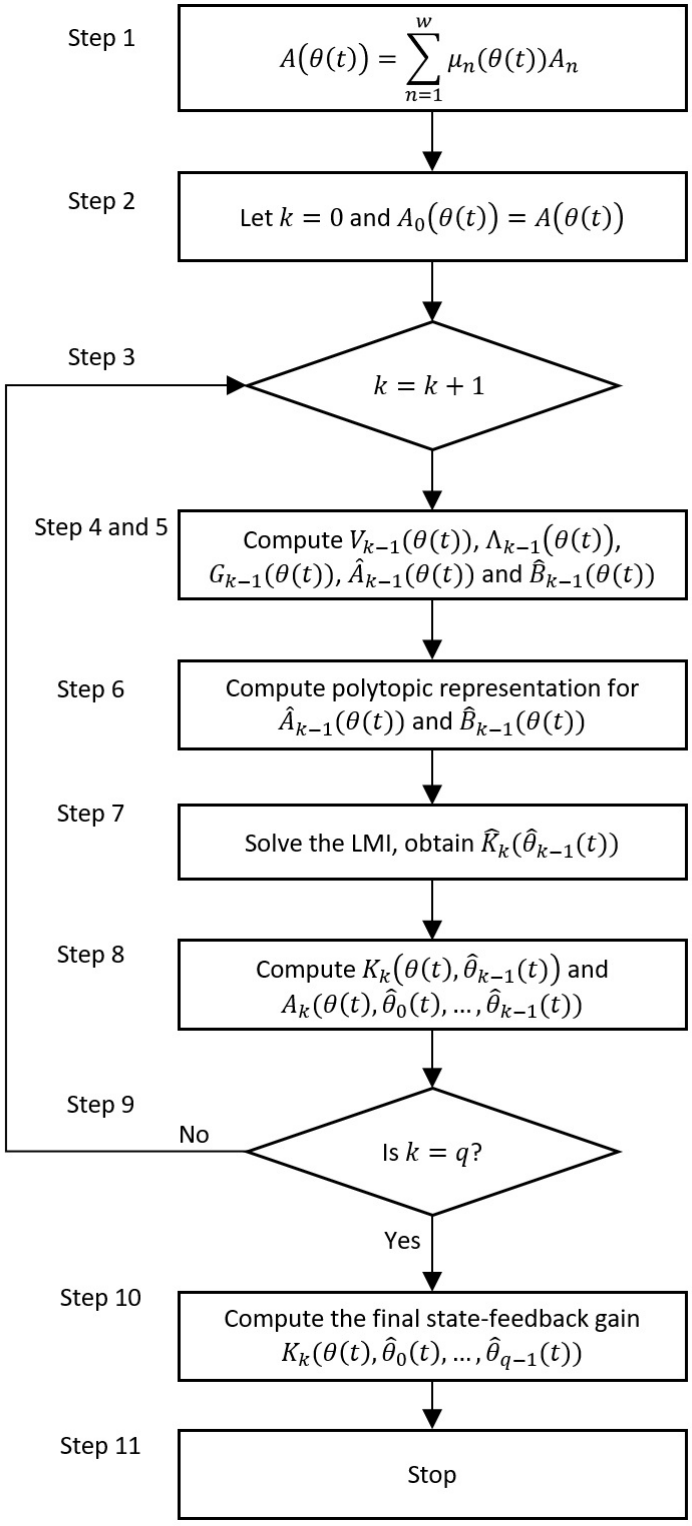

Figure 1. Flowchart of Algorithm 1.

- **Step 5:** Use $\hat{A}_{k-1}(\theta(t))$ obtained from Step 5 in Algorithm 1 to compute the polytopic representation for $\hat{A}_{k-1}(\vartheta(t))$

$$\hat{A}_{k-1}(\vartheta(t)) = \hat{A}_{k-1}(\theta(t)) = \sum_{i=1}^{r} \alpha_{k-1,i}(\vartheta_{k-1}(t))\hat{A}_{k-1,i}. \tag{43}$$

- **Step 6:** Use $\hat{K}_k(\hat{\theta}_{k-1}(t))$ obtained from Step 7 in Algorithm 1 to compute the partial controller gain:

$$\hat{K}_k(\vartheta(t)) = \hat{K}_k(\hat{\theta}_{k-1}(t)) = \sum_{i=1}^{r} \alpha_{k-1,i}(\vartheta_{k-1}(t))\hat{K}_{k,i}. \tag{44}$$

- **Step 7:** Compute the state feedback gain as

$$K_k(\vartheta(t)) = \hat{K}_k(\vartheta(t))G_{k-1}(\vartheta(t)) \tag{45}$$

  and the closed-loop matrix as:

$$A_k(\vartheta(t)) = A_{k-1}(\vartheta(t)) + B(\vartheta(t))K_k(\vartheta(t)) \tag{46}$$

- **Step 8:** If $k \neq q$ then go to **Step 3**
- **Step 9:** The final state-feedback gain that achieves the desired pole clustering in the specified union of regions is given by:

$$K(\vartheta(t)) = \sum_{k=1}^{q} K_k(\vartheta(t)) \tag{47}$$

- **Step 10:** Stop

Remark 1: Note that if a solution to the LMI feasibility problem exists, then available LMI solvers would be able to return a solution within a finite time, albeit possible numerical issues that could arise, for example, from the matrix $V(\theta(t))$ being close to singular for some value of θ.

Remark 2: A limitation of the proposed algorithm is that it is not possible to know beforehand, the feasibility of the linear matrix inequalities, which depend on the desired regions' location and area. To address this fact, it is recommended to run the algorithm multiple times, choosing in the first attempts big regions in which the poles are to be placed, and then fine-tuning the results by considering progressively smaller regions.

Remark 3: A drawback of the proposed algorithm is that it introduces some computational burden when compared to the traditional pole placement approach. However, it is worth noting that moving a reduced number of poles requires LMIs with a smaller size, which compensates somehow the increase of complexity of the algorithm. The interested reader is referred to Appendix C for a comparison of computation times between the proposed LPV pole clustering approach and the traditional pole placement approach (Nguang & Shi, 2006). R6-4

4. Shifting pole clustering

4.1. $\mathcal{D}_R(\theta(t))$-stability for LPV systems

In this section, a shifting pole clustering approach for LPV system is introduced, which is inspired by the ideas in Rotondo et al. (2013), where a state-feedback controller was designed for LPV system using shifting pole placement. This section will extend this approach to partial pole clustering into the union of regions. Unlike the approach discussed in Section 3, hereafter we consider the case in which the LMI region is scheduled by the varying parameter, which means that the considered region is some $\mathcal{D}(\theta(t))$, obtained through subsets of the complex plane $\mathcal{D}_R(\theta(t))$ defined according to:

$$\mathcal{D}_R(\theta(t)) = \{s \in \mathbb{C} : R_{00}(\theta(t)) + (R_{10}(\theta(t))s)^H + R_{11}(\theta(t))s^*s \prec 0\}, \tag{48}$$

where $R(\theta(t))$ is a $2d \times 2d$ Hermitian matrix given by:

$$R(\theta(t)) = \begin{bmatrix} R_{00}(\theta(t)) & R_{10}(\theta(t)) \\ R_{10}(\theta(t))^* & R_{11}(\theta(t)) \end{bmatrix} \in \mathbb{C}^{2d\times 2d}, \theta \in \Theta. \tag{49}$$

If the $\mathcal{D}_R(\theta(t))$-stability of the LPV system (11) is considered, then the inequality (23) becomes:

$$R_{00}(\theta(t)) \otimes P + (R_{10}(\theta(t)) \otimes (PA(\theta(t))))^H + R_{11}(\theta(t)) \otimes (A(\theta(t))^* PA(\theta(t))) \prec 0 \tag{50}$$

and for partial pole placement in $\mathcal{D}_R(\theta(t))$, the aggregated state-feedback gain $\hat{K}(\theta(t))$ has to be chosen in such way that it satisfies:

$$\begin{aligned} &R_{00}(\theta(t)) \otimes \hat{P} + (R_{10}(\theta(t)) \otimes (\hat{P}(\hat{A}(\theta(t)) + \hat{B}(\theta(t))\hat{K}(\theta(t)))))^H + ... \\ &+ R_{11}(\theta(t)) \otimes ((\hat{A}(\theta(t)) + \hat{B}(\theta(t))\hat{K}(\theta(t)))^* \hat{P}(\hat{A}(\theta(t)) + \hat{B}(\theta(t))\hat{K}(\theta(t)))) \prec 0 \end{aligned} \tag{51}$$

for some matrix $\hat{P} \succ 0$.

The following theorem provides the parameter-dependent LMIs required to achieve partial pole clustering in the shifting $\mathcal{D}_R(\theta)$-region.

Theorem 2: There exists an aggregated state-feedback gain $\hat{K}(\theta)$ that assigns p eigenvalues in the region $\mathcal{D}_R(\theta)$ defined by (48) if there exist a matrix $\hat{X} \succ 0$ and a matrix $\hat{S}(\theta)$ such that $\forall \theta \in \Theta$:

$$\begin{bmatrix} R_{00}(\theta) \otimes \hat{X} + (R_{10}(\theta) \otimes (\hat{A}(\theta)\hat{X} + \hat{B}(\theta)\hat{S}(\theta)))^H & Z^*(\theta) \otimes (\hat{A}(\theta)\hat{X} + \hat{B}(\theta)\hat{S}(\theta))^* \\ Z(\theta) \otimes (\hat{A}(\theta)\hat{X} + \hat{B}(\theta)\hat{S}(\theta)) & -I_d \otimes \hat{X} \end{bmatrix} \prec 0, \tag{52}$$

where $Z(\theta)$ is given by the parameter-varying Cholesky factorization $R_{11}(\theta) = Z^*(\theta)Z(\theta)$, then the aggregated feedback gain is given by (26).

Proof: This theorem is a modification of Theorem 1, in which the matrices describing the $\mathcal{D}_R$-region are allowed to vary according to the varying parameter $\theta(t)$. □

It is necessary to mention that due to the varying nature of $R(\theta(t))$, there would appear triple summations due to terms such as $R_{10}(\theta(t)) \otimes \hat{P}(\hat{A}(\theta(t)) + \hat{B}(\theta(t))\hat{K}(\theta(t)))^H$. These terms can be handled using Polya's theorem, as done in Corollary 1 for the case of double summations, obtaining sufficient conditions that become progressively less conservative and eventually necessary. The details are omitted. Note that, by looking

at (5)-(6), it is possible to constrain $R_{10}(\theta)$ and $R_{11}(\theta)$ to be constant, and still obtain parameter-varying vertical half-planes or disks with a fixed center but a parameter-varying radius, which can be used to change online the closed-loop performance while reducing triple summations into double summations, thus simplifying the application of Polya's theorem.

4.2. Shifting pole clustering in a union of $\mathcal{D}_R(\theta(t))$-regions for LPV system

Assume the region of interest $\mathcal{D}(\theta(t))$ to be defined as follows:

$$\mathcal{D}(\theta(t)) = \bigcup_{k=1}^{q} \mathcal{D}_{R_k}(\theta(t)), \tag{53}$$

where each subregion $\mathcal{D}_{R_k}(\theta(t))$ is a region defined as in (48). Then, the shifting pole clustering in $\mathcal{D}(\theta(t))$ can be performed by successive partial pole placement in the subregions $\mathcal{D}_{R_k}(\theta(t))$, for $k = 1, ..., q$, where $R_k(\theta(t))$ must be constrained to vary polytopically in order to obtain a finite number of conditions which can be solved computationally:

$$R_k(\theta(t)) = \sum_{n=1}^{w} \mu_n(\theta(t)) R_{k,n}. \tag{54}$$

The shifting pole clustering in a union of $\mathcal{D}_R(\theta(t))$-regions is achieved through the algorithm introduced in Section 3.3, the main differences being the following:

- At **Step 1**, additionally consider the varyingness of the regions as in (54).
- In **Step 6**, a new polytopic representation for $R_k(\theta(t))$ in terms of the new scheduling vector $\hat{\theta}_{k-1}$:

$$R_k(\theta(t)) = R_k(\hat{\theta}_{k-1}(t)) = \sum_{i=1}^{r} \alpha_{k-1,i}(\hat{\theta}_{k-1}(t)) R_{k,i} \tag{55}$$

  must be sought. An approximate solution can be found by considering the actual values of $R_k(\theta(t))$ for several values of $\theta(t)$ as if they were known measurements, while the matrices $R_{k,i}$ are unknown parameters to be estimated using estimation techniques, e.g., *least-squares*. Further details about this point are provided in connection with the example in Section 5.1.2.
- At **Step 7**, the LMI (52) should hold, with $R(\theta(t))$ replaced by $R_k(\theta(t))$.

5. Simulation results

5.1. Numerical example

5.1.1. $\mathcal{D}_R$-stabilization in a union of $\mathcal{D}_R$-regions

Let us consider a polytopic LPV system as in (12) with matrices given by:

$$A_1 = \begin{bmatrix} 2.05 & -15.93 & 15.32 \\ 40.47 & -326.56 & 298.17 \\ 44.86 & -359.16 & 327.50 \end{bmatrix}, \quad A_2 = \begin{bmatrix} 15.86 & -44.81 & 41.76 \\ 53.22 & -361.51 & 335.84 \\ 56.30 & -388.59 & 360.65 \end{bmatrix}, \quad B = \begin{bmatrix} 1 \\ 0 \\ 0 \end{bmatrix},$$

where $A(\theta(t))$ depends on the varying parameters $\theta(t) \in [0, 1]$ as follows:

$$A(\theta(t)) = \mu_1(\theta(t))A_1 + \mu_2(\theta(t))A_2, \tag{56}$$

with:

$$\mu_1(\theta(t)) = \theta(t), \quad \mu_2(\theta(t)) = 1 - \theta(t).$$

The system is clearly open-loop unstable since its frozen poles are all located in the right half-plane, as shown in Fig. 2.

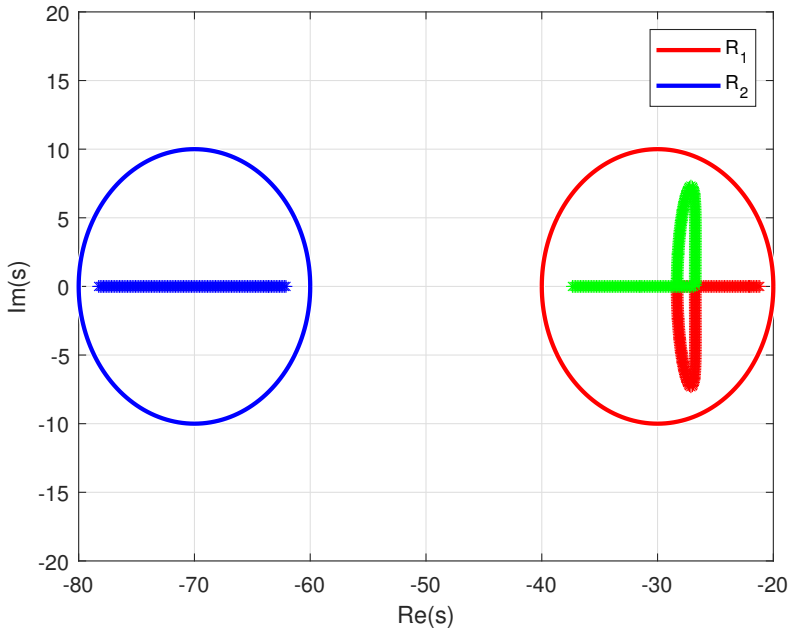

Figure 2. Position of the open-loop frozen poles for $\theta \in [0, 1]$.

Pole clustering is performed as follows: at iteration $k = 1$, the two conjugate poles are moved to $\mathcal{D}_{R_1}$; then, at iteration $k = 2$, the remaining open-loop unstable real pole is moved to $\mathcal{D}_{R_2}$. The mentioned regions $\mathcal{D}_{R_1}$ and $\mathcal{D}_{R_2}$ are selected as disks with predetermined center and radius, as listed in Table 1.

The design is performed using two different sets of regions, with $\mathcal{D}_1$ located closer

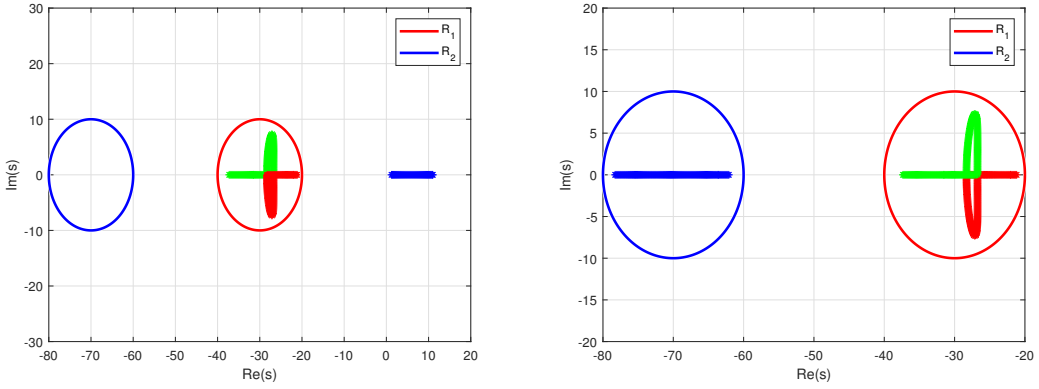

(a) Poles position in $\mathcal{D}_1$ at iteration $k = 1$

(b) Poles position in $\mathcal{D}_1$ at iteration $k = 2$

Figure 3. Position of the closed-loop frozen poles in region $\mathcal{D}_1$.

to the imaginary axis (hence, corresponding to a slower time response), whereas $\mathcal{D}_2$ is located farther (thus corresponding to a faster response). Note that Table 1 provides also another set of regions, denoted as $\mathcal{D}_3$, which will be considered later, in the next subsection, for the sake of illustrating the shifting pole clustering technique.

Table 1. Parameter chosen for controller design.

	Center of $\mathcal{D}_{R_1}$	Radius of $\mathcal{D}_{R_1}$	Center of $\mathcal{D}_{R_2}$	Radius of $\mathcal{D}_{R_2}$
$\mathcal{D}_1$	$(-30, 0)$	10	$(-70, 0)$	10
$\mathcal{D}_2$	$(-50, 0)$	17	$(-100, 0)$	17
$\mathcal{D}_3$	$(-50, 0)$	17	$(-150, 0)$	17

The controller design is performed by applying Algorithm introduced in Section 3.3. It is worth mentioning that, in Step 6 of the algorithm, after computing $\hat{A}_{k-1}$ and $\hat{B}_{k-1}$, the new scheduling vector $\hat{\theta}_{k-1}$ has been obtained by choosing the elements of $\hat{A}_{k-1}$ and $\hat{B}_{k-1}$ as varying parameters, and the corresponding polytopic representation with matrices $\hat{A}_{k-1,i}$ and $\hat{B}_{k-1,i}$ has been obtained by applying the approach commonly referred to in the literature as *bounding box*, i.e. by considering different combinations of the maximum and minimum values of each element of $\hat{A}_{k-1}$ and $\hat{B}_{k-1}$. The interested reader will find the values of $\hat{A}_{k-1,i}$, $\hat{B}_{k-1,i}$, together with the $\hat{K}_{k,i}$ obtained in step 7 of the algorithm, reported in the Appendix.

Fig. 3(a) shows that after the iteration $k = 1$ of the algorithm, the two conjugate poles (in the frozen parameter-varying sense) are moved into the first subregion of $\mathcal{D}_{R_1}$, while the third parameter-varying pole is kept at the original location. Fig. 3(b) shows that at iteration $k = 2$ of the algorithm, the third pole is eventually moved to the second subregion of $\mathcal{D}_{R_2}$.

Fig. 4 shows the same process as Fig. 3 but moving the poles to region $\mathcal{D}_2$ which is located farther than $\mathcal{D}_1$.

In order to validate the obtained control law, let us perform simulations starting from the initial condition:

$$x(0) = \begin{bmatrix} 5 & -5 & 5 \end{bmatrix}^T.$$

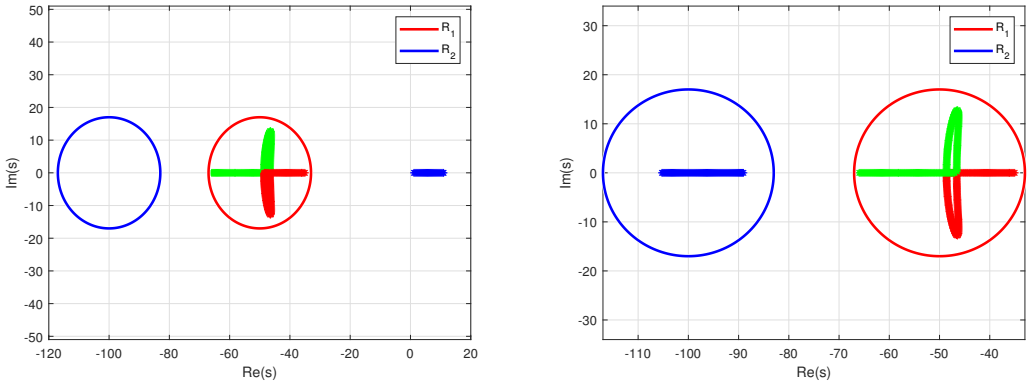

(a) Poles position in $\mathcal{D}_2$ at iteration $k = 1$

(b) Poles position in $\mathcal{D}_2$ at iteration $k = 2$

Figure 4. Position of the closed-loop frozen poles in region $\mathcal{D}_2$.

Fig. 5 shows the closed-loop response by applying the designed state-feedback control law. It is clear that if the dominant poles are farther from the imaginary axis, the system converges to zero faster, i.e. the convergence of the states with chosen region $\mathcal{D}_2$ is faster than with region $\mathcal{D}_1$, as it would be predicted by LTI considerations about the pole location.

5.1.2. Shifting $\mathcal{D}_R(\theta(t))$-stabilization in a union of parameter-varying $\mathcal{D}_R$-regions

In this section, the previously described numerical system is considered for the implementation of the shifting approach described in Section 4. In order to keep the mathematical complexity simple, we consider that only the radius of the disks of interest varies depending on the value of the scheduling parameter $\theta(t)$, which means that:

$$R_k(\theta(t)) = \begin{bmatrix} c_1^2 + c_2^2 - r_k(\theta(t))^2 & -c_1 + c_2 i \\ -c_1 - c_2 i & 1 \end{bmatrix}$$

with $r_k(\theta(t))$ defined as:

$$r_1(\theta(t)) = (1 + 1.2\theta(t))r_{1,0}, \tag{57}$$
$$r_2(\theta(t)) = (1 + 3\theta(t))r_{2,0}, \tag{58}$$

where $r_{k,0}$ denotes the values of the radii denoted as $\mathcal{D}_3$ in Table 1.

It is worth mentioning that, after obtaining the polytopic matrices $\hat{A}_{k-1,i}$ and $\hat{B}_{k-1,i}$ at step 6 of the algorithm, in terms of the new varying parameter $\hat{\theta}_{k-1}$, it is necessary to describe the variation of the regions of interest $R_k(\theta(t))$ in terms of $\hat{\theta}_{k-1}(t)$ as well as possible. Although an exact solution to this problem, in general, does not exist, an approximate solution can be found by fitting the following equation:

$$r_k(\theta(t))^2 = \sum_{i=1}^{r} \alpha_{k-1,i}(\hat{\theta}_{k-1}(t)) \cdot \beta_{k-1,i}(\hat{\theta}_{k-1}(t)) + \beta_{k-1,0} \tag{59}$$

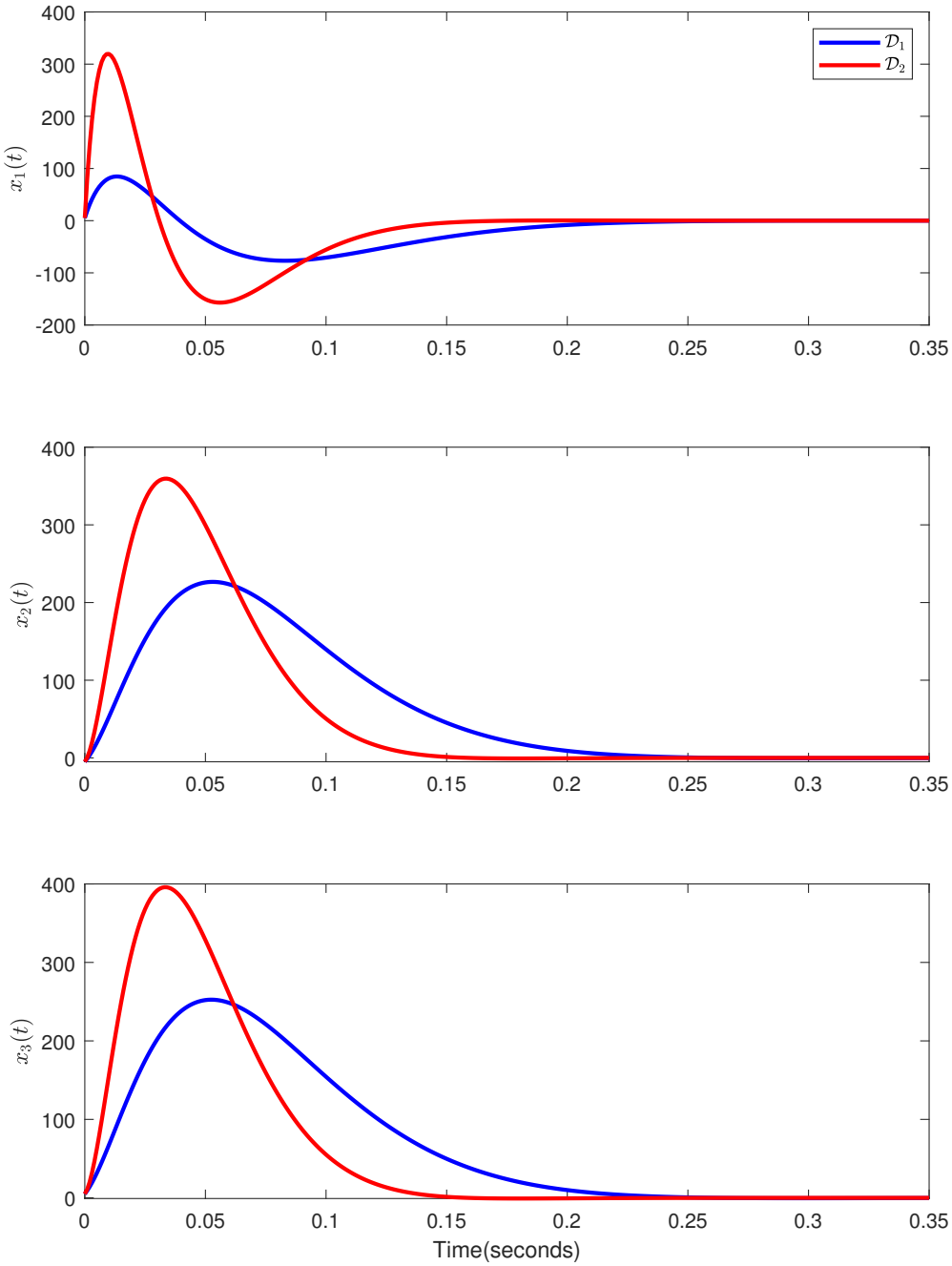

Figure 5. The closed-loop response by pole clustering in $\mathcal{D}_1$ (blue) and $\mathcal{D}_2$ (red).

in the least-squares sense, using as input data $(\alpha_{k-1,i}(\hat{\theta}_{k-1}(t)); r_k(\theta(t))^2)$ where $\alpha_{k-1,i}(\hat{\theta}(t))$ are the known coefficients of the polytopic decomposition obtained beforehand and $r_k(\theta(t))^2$ is the radius of the circular region $R_k(\theta(t))$. The coefficient vector $\beta_{k-1} = [\ \beta_{k-1,0} \quad \beta_{k-1,1} \quad \cdots \quad \beta_{k-1,r}\ ]^T$ is then computed as:

$$\beta_{k-1} = \begin{bmatrix} I & \alpha_{k-1} \end{bmatrix}^+ r_k(\theta(t))^2. \tag{60}$$

Fig. 6 shows the frozen-parameter poles position after shifting pole clustering in $\mathcal{D}_3$, where the circles in red correspond to $R_k(\theta(t))$ when $\theta = 0$ while those in blue to $R_k(\theta(t))$ when $\theta = 1$. It can be seen that as θ increases, the region become bigger and the variation of the poles getting wider, however the poles are still located inside the region. At $\theta = 1$, it allows wider region of the poles, when $\theta = 0$, a more precise performance requirement is obtained. Moreover, Fig.7 shows that the desired regions and the actual positions of the closed-loop poles vary according to the value of θ.

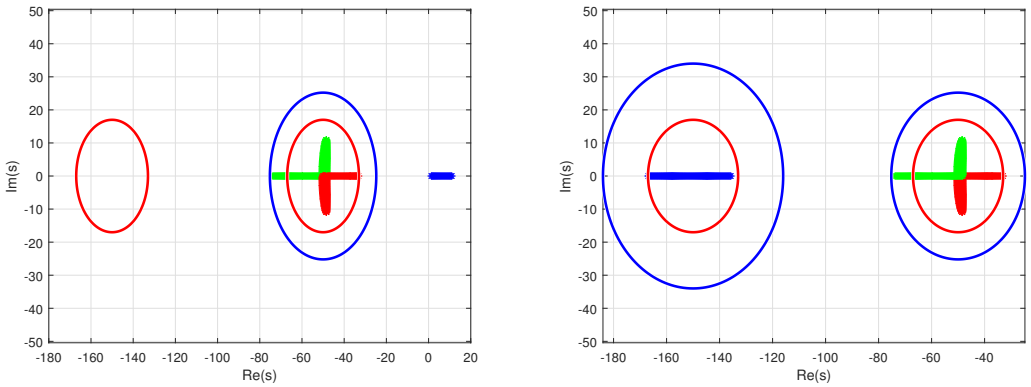

(a) Poles position in $\mathcal{D}_3$ at iteration $k = 1$

(b) Poles position in $\mathcal{D}_3$ at iteration $k = 2$

Figure 6. Position of the closed-loop frozen poles using the shifting pole clustering approach.

Fig. 8 shows that the behavior of the closed-loop state variables depends upon the trajectory of θ. These responses have been obtained starting from the initial state $x(0) = \begin{bmatrix} -5.6 & 5.4 & 6.1 \end{bmatrix}^T$ in four different cases, three of which corresponding to constant values of the scheduling parameter $\theta = 0.2$, $\theta = 0.6$ and $\theta = 1$ (red, green and blue line, respectively), and the remaining case corresponding to a time-varying scheduling parameter trajectory as follows: $\theta(t) = 0.6 - 0.4\cos(5\pi t)$ (purple line). It can be seen from the figure that the closed-loop system behaves as expected, in the sense that for the value of θ which corresponds to poles located farther from the imaginary axis, a faster dynamics of the closed-loop system is obtained. The purple curve shows that at the beginning of the simulation, the system behaves in an underdamped way due to the value of the varying parameter being approximately equal to $\theta = 0.2$ (exactly equal at $t = 0$); then, as the value of $\theta(t)$ increases with time, the closed-loop frozen pole get closer to the real axis, which increases the damping and causes the oscillations to fade away.

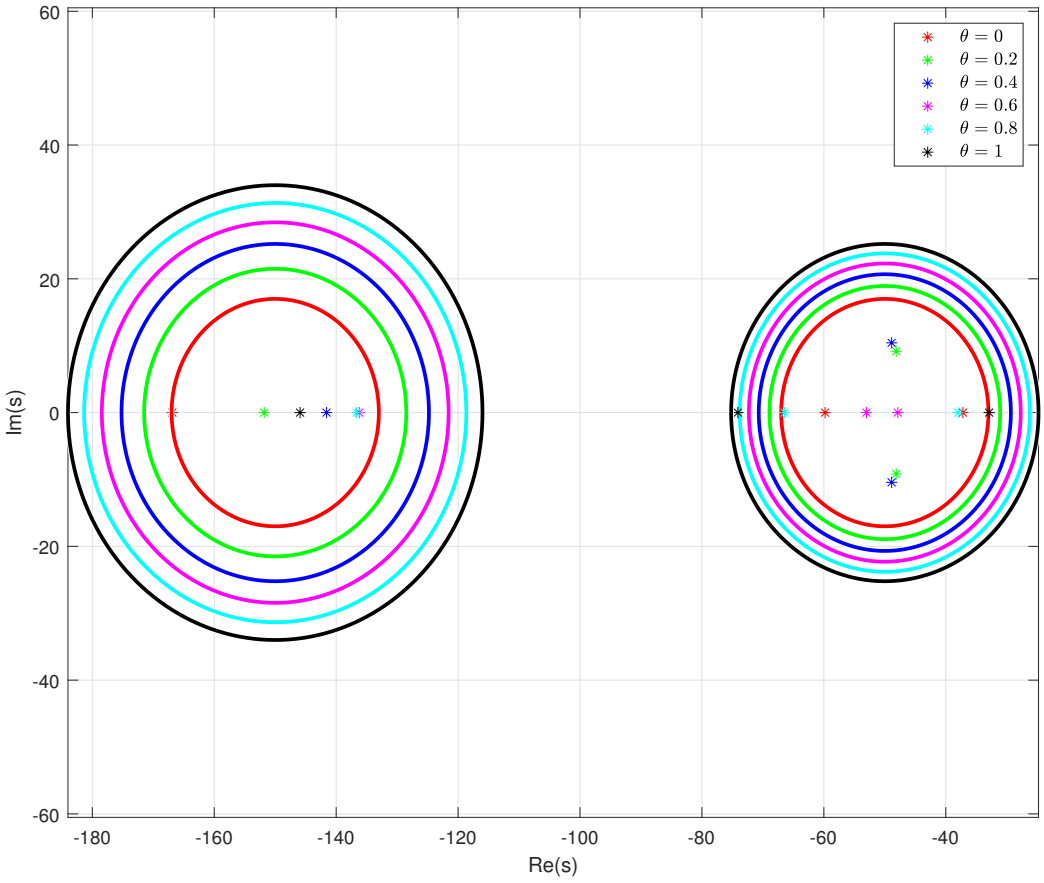

Figure 7. Position of the closed-loop poles for different values of θ using the shifting approach.

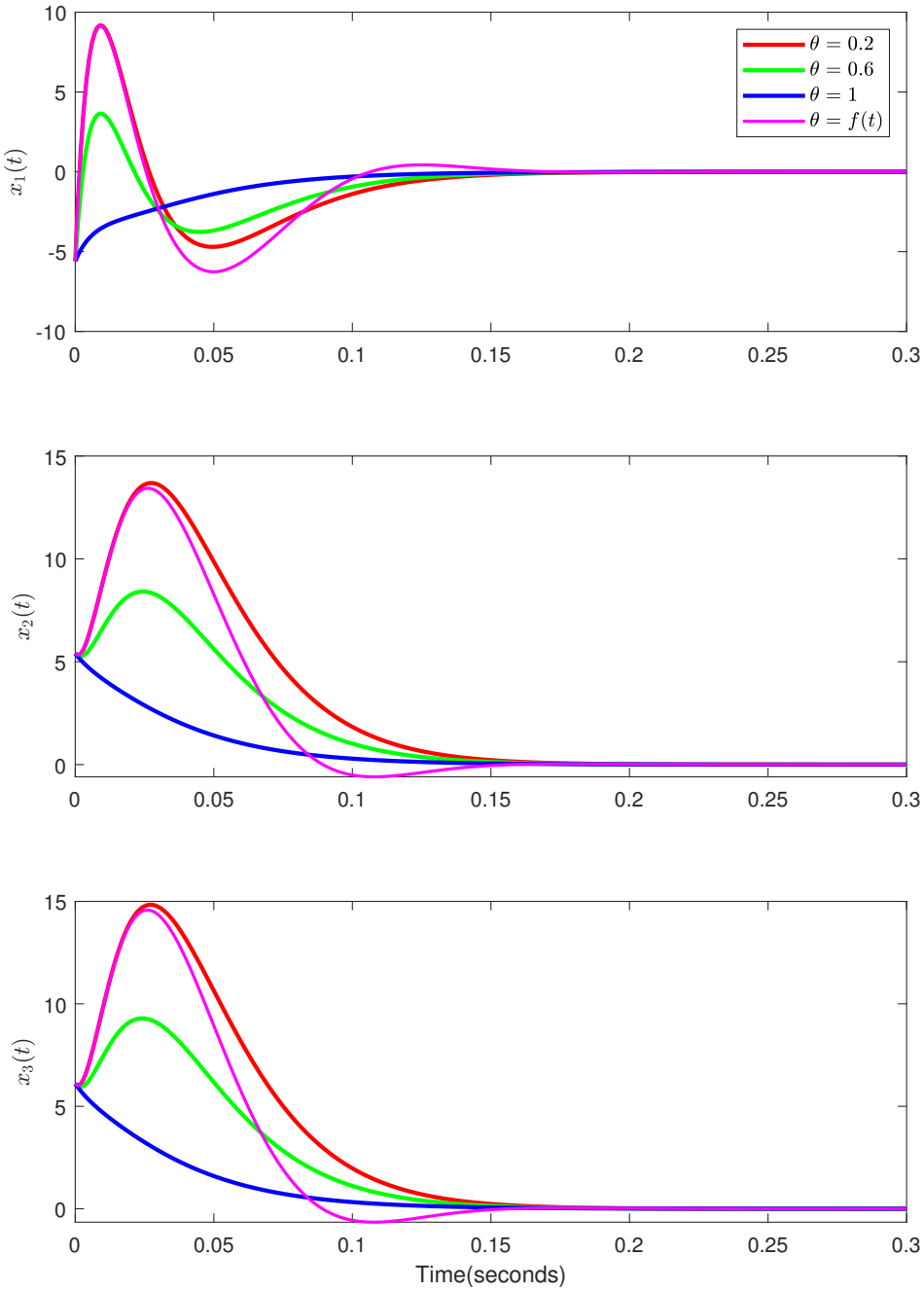

Figure 8. System response for different values/trajectories of $\theta(t)$ using the shifting approach.

5.2. Application to a two-tank system simulator

The goal of this section is to show an application to a system often used as a validation setup in real control applications, i.e., a two-tank system. This system is made up of two-tanks as shown in Fig. 9. It contains two coupled cylindrical tanks connected by

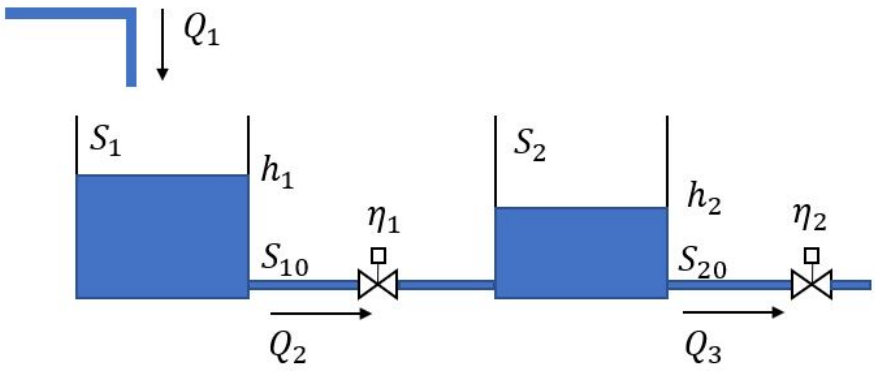

Figure 9. Two-tank system.

a pipe. The cross-sectional areas of tank 1 and tank 2 are given by $S_1 = S_2 = 2m^2$. Liquid is filled into the tank 1 by the pump, whose input flow is denoted as Q_1. On the other hand, Q_2 is the flow of liquid through a connecting pipe with cross-section $S_{10} = 0.6m^2$, Q_3 is the output flow of liquid from the tank 2 with cross-section $S_{20} = 0.5m^2$, both pipes are affected by the valves described by coefficients η_1 and η_2, which are outflow coefficients for tank 1 and tank 2, respectively. It is assumed that the parameters η_1 and η_2 vary over time, although their instantaneous value is known and can be used to perform the LPV scheduling. The state variables for this system are the liquid levels in both tanks: h_1, h_2 .

In the following, we consider the time-varying system obtained from the linearization of the nonlinear model about an equilibrium point (the time-varyingness comes from the variation of the valve coefficients due, e.g., to opening/closing the valves), corresponding to $Q_1 = Q_{1p}$ and desired liquid levels in individual tanks $h_1 = 2.4m$, $h_2 = 1.4m$. So, we obtain

$$S_1 \frac{d\Delta h_1(t)}{dt} = \Delta Q_1(t) - c_1(t)(\Delta h_1(t) - \Delta h_2(t)), \tag{61}$$

$$S_2 \frac{d\Delta h_2(t)}{dt} = c_1(t)(\Delta h_1(t) - \Delta h_2(t)) - c_2(t)\Delta h_2(t), \tag{62}$$

where

$$c_1(t) = \frac{1}{\sqrt{2}}\eta_1(t)S_{10}\sqrt{\frac{g}{h_1 - h_2}}, \quad c_2(t) = \frac{1}{\sqrt{2}}\eta_2(t)S_{20}\sqrt{\frac{g}{h_2}}.$$

Equations (61) and (62) can be formulated in the state-space as

$$\begin{bmatrix}\Delta\dot{h}_1(t)\\ \Delta\dot{h}_2(t)\end{bmatrix} = \begin{bmatrix}-\dfrac{c_1(t)}{S_1} & \dfrac{c_1(t)}{S_1}\\ \dfrac{c_1(t)}{S_2} & -\dfrac{c_1(t)+c_2(t)}{S_2}\end{bmatrix}\begin{bmatrix}\Delta h_1(t)\\ \Delta h_2(t)\end{bmatrix} + \begin{bmatrix}\dfrac{1}{S_1}\\ 0\end{bmatrix}\Delta Q_1(t), \tag{63}$$

$$y(t) = \begin{bmatrix}0 & 1\end{bmatrix}\begin{bmatrix}\Delta h_1(t) & \Delta h_2(t)\end{bmatrix}^T. \tag{64}$$

In the following we assume that the outflow coefficients can take values in the intervals $\eta_1 \in [0.37, 0.7]$ and $\eta_2 \in [0.37, 0.7]$, which lead to

$$\eta_{1max} = 0.7, \quad \eta_{1min} = 0.37, \quad \eta_{2max} = 0.7, \quad \eta_{2min} = 0.37,$$

so that the polytopic LPV system is given by:

$$A_1 = \begin{bmatrix}-0.4649 & 0.4649\\ 0.4649 & -0.7922\end{bmatrix}, \quad A_2 = \begin{bmatrix}-0.4649 & 0.4649\\ 0.4649 & -0.6379\end{bmatrix},$$
$$A_3 = \begin{bmatrix}-0.2457 & 0.2457\\ 0.2457 & -0.5731\end{bmatrix}, \quad A_4 = \begin{bmatrix}-0.2457 & 0.2457\\ 0.2457 & -0.4188\end{bmatrix}.$$

$$B = \begin{bmatrix}0.5 & 0\end{bmatrix}^T,$$

where $A(\theta(t))$ depends on the varying parameters $\theta_1(t), \theta_2(t) \in [0, 1]$ as follows:

$$A(\theta(t)) = \mu_1(\theta(t))A_1 + \mu_2(\theta(t))A_2 + \mu_3(\theta(t))A_3 + \mu_4(\theta(t))A_4, \tag{65}$$

with:

$$\mu_1(\theta(t)) = \theta_1(t)\theta_2(t), \quad \mu_2(\theta(t)) = \theta_1(t)(1-\theta_2(t)),$$
$$\mu_3(\theta(t)) = (1-\theta_1(t))\theta_2(t), \quad \mu_4(\theta(t)) = (1-\theta_1(t))(1-\theta_2(t)).$$

The two-tank system is open-loop stable and its frozen poles are all located in the left half-plane, as shown in Fig. 10.

Pole clustering is performed similarly as previous example, the region $\mathcal{D}_{R_4}$ and $\mathcal{D}_{R_5}$ selected as disks with predetermined center and radius, as listed in Table 2.

Table 2. Parameter chosen for controller design.

	Center of $\mathcal{D}_{R_1}$	Radius of $\mathcal{D}_{R_1}$	Center of $\mathcal{D}_{R_2}$	Radius of $\mathcal{D}_{R_2}$
$\mathcal{D}_4$	$(-8, 0)$	1.6	$(-4, 0)$	1.6
$\mathcal{D}_5$	$(-11, 0)$	2	$(-6, 0)$	2

Fig. 11(a) shows after iteration $k = 1$ of the algorithm, the first pole is moved to the the disk on the left $\mathcal{D}_{R_1}$, then in Fig. 11(b) at $k = 2$, the remaining pole is moved to $\mathcal{D}_{R_2}$. Fig. 12 shows the same process but moving the poles to $\mathcal{D}_5$.

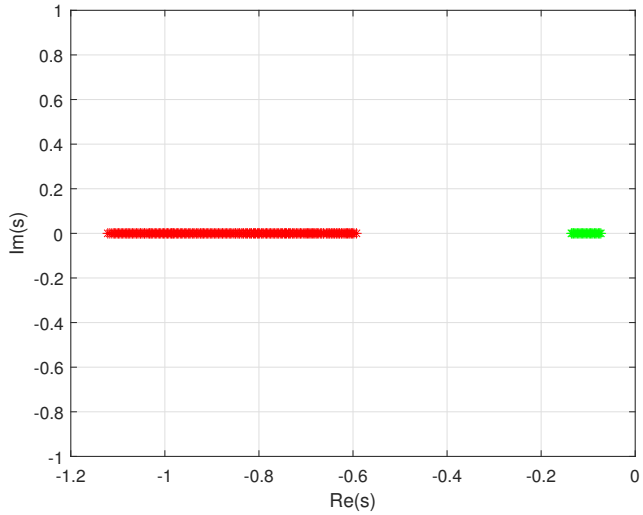

Figure 10. Position of the open-loop frozen poles for $\theta_1, \theta_2 \in [0, 1]$.

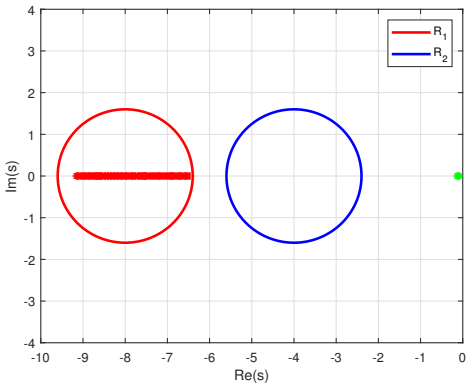

(a) Poles position in $\mathcal{D}_4$ at iteration $k = 1$

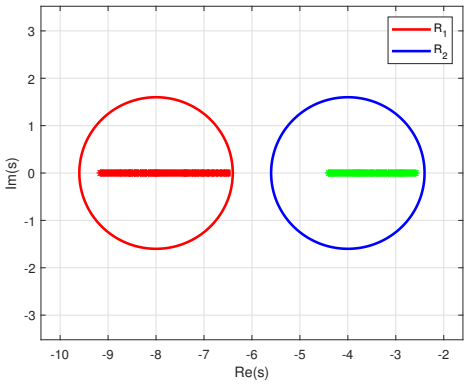

(b) Poles position in $\mathcal{D}_4$ at iteration $k = 2$

Figure 11. Position of the closed-loop frozen poles in region $\mathcal{D}_4$.

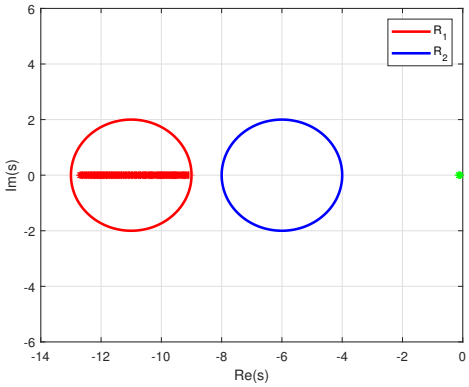

(a) Poles position in $\mathcal{D}_5$ at iteration $k = 1$

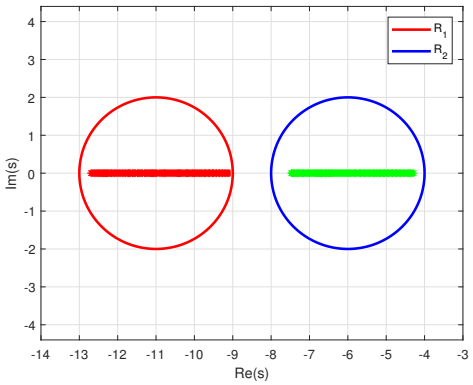

(b) Poles position in $\mathcal{D}_5$ at iteration $k = 2$

Figure 12. Position of the closed-loop frozen poles in region $\mathcal{D}_5$.

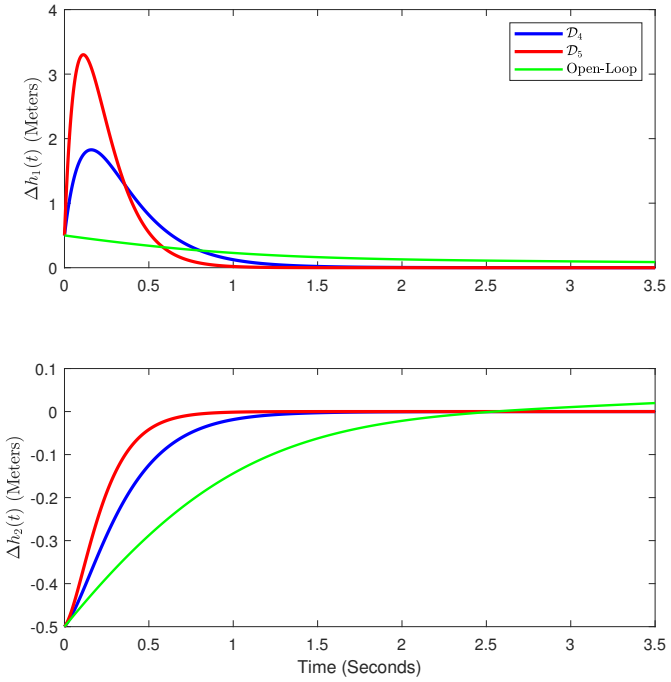

Figure 13. The closed-loop response by pole clustering in $\mathcal{D}_4$ (blue), $\mathcal{D}_5$ (red) and the open-loop response (green).

For validating the obtained control law, let us perform simulations starting from the initial condition:

$$\Delta h(0) = \begin{bmatrix} 0.5\,m & -0.5\,m \end{bmatrix}^T$$

Fig. 13 shows the closed-loop response by applying the designed state-feedback control law. It is clear the convergence of the state is faster under the controller whose poles are farther from the imaginary axis. Meanwhile, the green line represents the open-loop response.

6. Conclusions

This paper has provided a procedure for pole clustering in a union of $\mathcal{D}_R$-regions for LPV systems. From this technique, a method to compute a state-feedback gain that achieves the desired closed-loop pole location has been deduced. Furthermore, this technique has been extended to the shifting case, thus allowing pole clustering in parameter-dependent varying regions which enables online modification of the transient performance. The proposed technique has been validated in simulation using a numerical system and a two-tank system, demonstrating the main characteristics and the effectiveness of the developed control strategy. Future work will be devoted to developing equivalent techniques for LPV systems with residual nonlinearities, such as parameter-varying Lipschitz or quadratic terms, or the systems with disturbances or uncertainties, such as the application proposed in Gao, Sun, Liu, Shi, and Wu (2020)

and Gao, Li, Wu, Karimi, and Lam (2016).

Funding

This work has been funded by the Spanish State Research Agency (AEI) and the European Regional Development Fund (ERFD) through the project SCAV (ref. MINECO DPI2017-88403-R), by the DGR of Generalitat de Catalunya (SAC group ref. 2017/SGR/482) and by SMART Project (ref. num. EFA153/16 Interreg Cooperation Program POCTEFA 2014-2020).

References

Bachelier, O., & Pradin, B. (1999). Bounds for uncertain matrix root-clustering in a union of subregions. *International Journal of Robust and Nonlinear Control: IFAC-Affiliated Journal*, *9*(6), 333–359.

Baranyi, P. (2009). Convex hull generation methods for polytopic representations of LPV models. In *2009 7th international symposium on applied machine intelligence and informatics* (pp. 69–74).

Blesa, J., Jiménez, P., Rotondo, D., Nejjari, F., & Puig, V. (2014). An interval NLPV parity equations approach for fault detection and isolation of a wind farm. *IEEE Transactions on Industrial Electronics*, *62*(6), 3794–3805.

Bosche, J., Bachelier, O., & Mehdi, D. (2005). An approach for robust matrix root-clustering analysis in a union of regions. *IMA Journal of Mathematical Control and Information*, *22*(3), 227–239.

Bouazizi, M., Kochbati, A. K., & Ksouri, M. (2001). LPV control of uncertain systems by observer with pole placement and H_2 constraints. *IFAC Proceedings Volumes*, *34*(13), 291–296.

Brizuela Mendoza, J. A., Sorcia Vázquez, F. D. J., Guzmán Valdivia, C., Osorio Sánchez, R., & Martínez García, M. (2018). Observer design for sensor and actuator fault estimation applied to polynomial LPV systems: A riderless bicycle study case. *International Journal of Systems Science*, *49*(14), 2996–3006.

Chesi, G. (2017). Parameter and controller dependent Lyapunov functions for robust $\mathcal{D}$-stability and robust performance controller design. *IEEE Transactions on Automatic Control*, *62*(9), 4798–4803.

Chilali, M., & Gahinet, P. (1996). H_∞ design with pole placement constraints: an LMI approach. *IEEE Transactions on automatic control*, *41*(3), 358–367.

Ding, B., Dong, J., & Hu, J. (2019). Output feedback robust MPC using general polyhedral and ellipsoidal true state bounds for LPV model with bounded disturbance. *International Journal of Systems Science*, *50*(3), 625–637.

El-Guindy, A., Schaab, K., Schürmann, B., Stursberg, O., & Althoff, M. (2017). Formal LPV control for transient stability of power systems. In *2017 ieee power & energy society general meeting* (pp. 1–5).

Fujimori, A., & Ljung, L. (2005). A polytopic modeling of aircraft by using system identification. In *2005 international conference on control and automation* (Vol. 1, pp. 107–112).

Gao, Y., Li, H., Wu, L., Karimi, H. R., & Lam, H.-K. (2016). Optimal control of discrete-time interval type-2 fuzzy-model-based systems with D-stability constraint and control saturation. *Signal Processing*, *120*, 409–421.

Gao, Y., Sun, G., Liu, J., Shi, Y., & Wu, L. (2020). State estimation and self-triggered control of CPSs against joint sensor and actuator attacks. *Automatica*, *113*, 108687.

Ghersin, A. S., & Sanchez-Peña. (2002). LPV control of a 6-DOF vehicle. *IEEE Transactions on Control Systems Technology*, *10*(6), 883–887.

Hoffmann, C., & Werner, H. (2014). A survey of linear parameter-varying control applications validated by experiments or high-fidelity simulations. *IEEE Transactions on Control Systems Technology*, *23*(2), 416–433.

Jabali, M. B. A., & Kazemi, M. H. (2017a). A new LPV modeling approach using PCA-based parameter set mapping to design a PSS. *Journal of advanced research*, *8*(1), 23–32.

Jabali, M. B. A., & Kazemi, M. H. (2017b). A new polytopic modeling with uncertain vertices and robust control of robot manipulators. *Journal of Control, Automation and Electrical Systems*, *28*(3), 349–357.

Larimore, W. E. (2013). Identification of nonlinear parameter-varying systems via canonical variate analysis. In *2013 american control conference* (pp. 2247–2262).

Li, J., & Yang, G.-H. (2019). Fuzzy descriptor sliding mode observer design: A canonical form-based method. *IEEE Transactions on Fuzzy Systems*, *28*(9), 2048–2062.

López-Estrada, F. R., Ponsart, J.-C., Theilliol, D., Zhang, Y., & Astorga-Zaragoza, C.-M. (2016). LPV model-based tracking control and robust sensor fault diagnosis for a quadrotor uav. *Journal of Intelligent & Robotic Systems*, *84*(1-4), 163–177.

López-Estrada, F.-R., Rotondo, D., & Valencia-Palomo, G. (2019). A review of convex approaches for control, observation and safety of linear parameter varying and Takagi-Sugeno systems. *Processes*, *7*(11), 814.

López-Estrada, F.-R., Santos-Estudillo, O., Valencia-Palomo, G., Gómez-Peñate, S., & Hernandez-Gutiérrez, C. (2020). Robust qLPV tracking fault-tolerant control of a 3 DOF mechanical crane. *Mathematical and Computational Applications*, *25*(3), 48.

Maamri, N., Bachelier, O., & Mehdi, D. (2006). Pole placement in a union of regions with prespecified subregion allocation. *Mathematics and Computers in Simulation*, *72*(1), 38–46.

Morato, M. M., Normey-Rico, J. E., & Sename, O. (2020). Model predictive control design for linear parameter varying systems: A survey. *Annual Reviews in Control*.

Nejjari, F., Puig, V., de Oca, S. M., & Sadeghzadeh, A. (2009). Robust fault detection for LPV systems using interval observers and zonotopes. In *Proceedings of the 48h ieee conference on decision and control (cdc) held jointly with 2009 28th chinese control conference* (pp. 1002–1007).

Nguang, S. K., & Shi, P. (2006). Robust H_∞ output feedback control design for fuzzy dynamic systems with quadratic $\mathcal{D}$-stability constraints: An LMI approach. *Information Sciences*, *176*(15), 2161–2191.

Nguyen, A.-T., Márquez, R., Guerra, T.-M., & Dequidt, A. (2017). Improved LMI conditions for local quadratic stabilization of constrained Takagi-Sugeno fuzzy systems. *International Journal of Fuzzy Systems*, *19*(1), 225–237.

Peaucelle, D., Arzelier, D., Bachelier, O., & Bernussou, J. (2000). A new robust D-stability condition for real convex polytopic uncertainty. *Systems & control letters*, *40*(1), 21–30.

Pérez-Estrada, A.-J., Osorio-Gordillo, G.-L., Alma, M., Darouach, M., & Olivares-Peregrino, V.-H. (2018). H_∞ generalized dynamic unknown inputs observer design for discrete LPV systems. application to wind turbine. *European Journal of Control*, *44*, 40–49.

Rabaoui, B., Hamdi, H., Braiek, N. B., & Rodrigues, M. (2020). A reconfigurable PID fault tolerant tracking controller design for LPV systems. *ISA transactions*, *98*, 173–185.

Rizvi, S. Z., Velni, J. M., Abbasi, F., Tóth, R., & Meskin, N. (2018). State-space LPV model identification using kernelized machine learning. *Automatica*, *88*, 38–47.

Rotondo, D. (2017). *Advances in gain-scheduling and fault tolerant control techniques*. Springer.

Rotondo, D., Fernandez-Canti, R. M., Tornil-Sin, S., Blesa, J., & Puig, V. (2016). Robust Fault Diagnosis of Proton Exchange Membrane Fuel Cells using a Takagi-Sugeno Interval Observer Approach. *International Journal of Hydrogen Energy*, *41*(4), 2875–2886.

Rotondo, D., & Johansen, T. A. (2018). Analysis and design of quadratic parameter varying (QPV) control systems with polytopic attractive region. *Journal of the Franklin Institute*, *355*(8), 3488–3507.

Rotondo, D., Nejjari, F., & Puig, V. (2013). A shifting pole placement approach for the design of parameter-scheduled state-feedback controllers. In *2013 european control conference (ecc)*

(pp. 1829–1834).
Rotondo, D., Nejjari, F., & Puig, V. (2014). Robust state-feedback control of uncertain LPV systems: An LMI-based approach. *Journal of the Franklin Institute*, *351*(5), 2781–2803.
Rotondo, D., Nejjari, F., & Puig, V. (2015). Design of parameter-scheduled state-feedback controllers using shifting specifications. *Journal of the Franklin Institute*, *352*(1), 93–116.
Rotondo, D., Puig, V., & Nejjari, F. (2016). On the analogies in control design of non-linear systems using LPV and Takagi-Sugeno models. In *Systems and control (icsc), 2016 5th international conference on* (pp. 225–230).
Rotondo, D., Puig, V., Nejjari, F., & Witczak, M. (2015). Automated generation and comparison of Takagi–Sugeno and polytopic quasi-LPV models. *Fuzzy Sets and Systems*, *277*, 44–64.
Rugh, W. J., & Shamma, J. S. (2000). Research on gain scheduling. *Automatica*, *36*(10), 1401–1425.
Ruiz, A., Rotondo, D., & Morcego, B. (2019). Design of state-feedback controllers for linear parameter varying systems subject to time-varying input saturation. *Applied Sciences*, *9*(17), 3606.
Ruiz, A., Rotondo, D., & Morcego, B. (2020). Shifting H_∞ linear parameter varying state-feedback controllers subject to time-varying input saturations. In *Proceedings of the ifac world congress (2020).*
Sala, A., & Ariño, C. (2007). Asymptotically necessary and sufficient conditions for stability and performance in fuzzy control: Applications of Polya's theorem. *Fuzzy sets and systems*, *158*(24), 2671–2686.
San Miguel, A., Puig, V., & Alenyà, G. (2019). Fault-tolerant control of a service robot using a LPV robust unknown input observer. In *2019 4th conference on control and fault tolerant systems (systol)* (pp. 207–212).
Shamma, J. S. (1988). *Analysis and design of gain scheduled control systems* (Unpublished doctoral dissertation). Massachusetts Institute of Technology.
Shamma, J. S. (2012). An overview of LPV systems. In *Control of linear parameter varying systems with applications* (pp. 3–26). Springer.
Shen, Y., Yu, J., Luo, G., & Mei, Y. (2017). Missile autopilot design based on robust LPV control. *Journal of Systems Engineering and Electronics*, *28*(3), 536–545.
Sun, X.-D., & Postlethwaite, I. (1998). Affine LPV modelling and its use in gain-scheduled helicopter control.
Takagi, T., & Sugeno, M. (1985). Fuzzy identification of systems and its applications to modeling and control. *IEEE Transactions on Systems, Man, and Cybernetics*(1), 116–132.
Tornil-Sin, S., Theilliol, D., Ponsart, J.-C., & Puig, V. (2010). Admissible model matching using $\mathcal{D}_R$-regions: Fault accommodation and robustness against FDD inaccuracies. *International Journal of Adaptive Control and Signal Processing*, *24*(11), 927–943.
Yang, D., Zong, G., & Karimi, H. R. (2019). H_∞ refined antidisturbance control of switched LPV systems with application to aero-engine. *IEEE Transactions on Industrial Electronics*, *67*(4), 3180–3190.
Yang, R., Rotondo, D., & Puig, V. (2019). $\mathcal{D}$-stable controller design for Lipschitz NLPV system. *IFAC-PapersOnLine*, *52*(28), 88–93.
Yu, Z., Chen, H., & Woo, P.-y. (2002). Gain scheduled LPV H_∞ control based on LMI approach for a robotic manipulator. *Journal of Robotic Systems*, *19*(12), 585–593.
Zhang, H., Zhang, G., & Wang, J. (2016). H_∞ observer design for LPV systems with uncertain measurements on scheduling variables: Application to an electric ground vehicle. *IEEE/ASME Transactions on Mechatronics*, *21*(3), 1659–1670.
Zhang, L., Jia, M.-Y., & Yang, H. (2020). Non-fragile memory feedback control for uncertain time-varying delay switched fuzzy systems with unknown nonlinear disturbance. *Journal of Control and Decision*, 1–20.
Zhenxing, G., & Jun, F. (2019). Robust LPV modeling and control of aircraft flying through wind disturbance. *Chinese Journal of Aeronautics*, *32*(7), 1588–1602.

Appendix A. Numerical values for pole clustering in $\mathcal{D}_1$

The matrices $\hat{A}_{k-1,i}$ and $\hat{B}_{k-1,i}$ in (39)-(40) during iteration of Algorithm 1 $k = 1$ are given as follows:

$$\hat{A}_{0,1} = \begin{bmatrix} 2 & -10 \\ 10.36 & 2 \end{bmatrix}, \quad \hat{A}_{0,2} = \begin{bmatrix} 2 & -10 \\ 10.36 & 1 \end{bmatrix}, \quad \hat{A}_{0,3} = \begin{bmatrix} 2 & -10 \\ 10 & 2 \end{bmatrix},$$
$$\hat{A}_{0,4} = \begin{bmatrix} 2 & -10 \\ 10 & 1 \end{bmatrix}, \quad \hat{A}_{0,5} = \begin{bmatrix} 2 & -10.36 \\ 10.36 & 2 \end{bmatrix}, \quad \hat{A}_{0,6} = \begin{bmatrix} 2 & -10.36 \\ 10.36 & 1 \end{bmatrix},$$
$$\hat{A}_{0,7} = \begin{bmatrix} 2 & -10.36 \\ 10 & 2 \end{bmatrix}, \quad \hat{A}_{0,8} = \begin{bmatrix} 2 & -10.36 \\ 10 & 1 \end{bmatrix}, \quad \hat{A}_{0,9} = \begin{bmatrix} 1 & -10 \\ 10.36 & 2 \end{bmatrix},$$
$$\hat{A}_{0,10} = \begin{bmatrix} 1 & -10 \\ 10.36 & 1 \end{bmatrix}, \quad \hat{A}_{0,11} = \begin{bmatrix} 1 & -10 \\ 10 & 2 \end{bmatrix}, \quad \hat{A}_{0,12} = \begin{bmatrix} 1 & -10 \\ 10 & 1 \end{bmatrix},$$
$$\hat{A}_{0,13} = \begin{bmatrix} 1 & -10.36 \\ 10.36 & 2 \end{bmatrix}, \quad \hat{A}_{0,14} = \begin{bmatrix} 1 & -10.36 \\ 10.36 & 1 \end{bmatrix}, \quad \hat{A}_{0,15} = \begin{bmatrix} 1 & -10.36 \\ 10 & 2 \end{bmatrix},$$
$$\hat{A}_{0,16} = \begin{bmatrix} 1 & -10.36 \\ 10 & 1 \end{bmatrix}.$$

$$\hat{B}_{0,1} = \begin{bmatrix} -0.43 \\ -0.10 \end{bmatrix}, \quad \hat{B}_{0,2} = \begin{bmatrix} -0.45 \\ -0.11 \end{bmatrix}, \quad \hat{B}_{0,3} = \begin{bmatrix} -0.43 \\ -0.11 \end{bmatrix}, \quad \hat{B}_{0,4} = \begin{bmatrix} -0.45 \\ -0.10 \end{bmatrix},$$

then, the obtained controller gains $\hat{K}_{k,i}$ are:

$$\hat{K}_{1,1} = \begin{bmatrix} 91.68 & 192.69 \end{bmatrix}, \quad \hat{K}_{1,2} = \begin{bmatrix} 91.97 & 187.00 \end{bmatrix}, \quad \hat{K}_{1,3} = \begin{bmatrix} 88.38 & 187.32 \end{bmatrix},$$
$$\hat{K}_{1,4} = \begin{bmatrix} 89.11 & 185.33 \end{bmatrix}, \quad \hat{K}_{1,5} = \begin{bmatrix} 91.44 & 191.78 \end{bmatrix}, \quad \hat{K}_{1,6} = \begin{bmatrix} 91.78 & 186.36 \end{bmatrix},$$
$$\hat{K}_{1,7} = \begin{bmatrix} 88.18 & 185.52 \end{bmatrix}, \quad \hat{K}_{1,8} = \begin{bmatrix} 89.03 & 184.72 \end{bmatrix}, \quad \hat{K}_{1,9} = \begin{bmatrix} 90.88 & 193.00 \end{bmatrix},$$
$$\hat{K}_{1,10} = \begin{bmatrix} 90.87 & 186.08 \end{bmatrix}, \quad \hat{K}_{1,11} = \begin{bmatrix} 88.27 & 191.49 \end{bmatrix}, \quad \hat{K}_{1,12} = \begin{bmatrix} 88.50 & 186.24 \end{bmatrix},$$
$$\hat{K}_{1,13} = \begin{bmatrix} 91.03 & 192.73 \end{bmatrix}, \quad \hat{K}_{1,14} = \begin{bmatrix} 90.89 & 185.82 \end{bmatrix}, \quad \hat{K}_{1,15} = \begin{bmatrix} 87.92 & 190.19 \end{bmatrix},$$
$$\hat{K}_{1,16} = \begin{bmatrix} 88.58 & 186.09 \end{bmatrix}.$$

During the iteration $k = 2$, the matrices $\hat{A}_{k-1,i}$, $\hat{B}_{k-1,i}$ and $\hat{K}_{k,i}$ are obtained as follows:

$$\hat{A}_{1,1} = 11, \quad \hat{A}_{1,2} = 1, \quad \hat{B}_{1,1} = 0.18, \quad \hat{B}_{1,2} = 0.16.$$

$$\hat{K}_{2,1} = -405.98, \quad \hat{K}_{2,2} = -343.60.$$

Appendix B. Numerical information of pole placement in $\mathcal{D}_2$

When the region of interest is the one denoted as $\mathcal{D}_2$ in Table 1, at iteration $k = 1$ of Algorithm 1, the matrices $\hat{A}_{k-1,i}$ and $\hat{B}_{k-1,i}$ have the same values as the ones previously shown for the case of $\mathcal{D}_1$. Then, the obtained controller gains $\hat{K}_{k,i}$ are as

follows:

$$\hat{K}_{1,1} = \begin{bmatrix} 102.96 & 549.39 \end{bmatrix}, \quad \hat{K}_{1,2} = \begin{bmatrix} 102.32 & 539.21 \end{bmatrix}, \quad \hat{K}_{1,3} = \begin{bmatrix} 99.73 & 539.80 \end{bmatrix},$$
$$\hat{K}_{1,4} = \begin{bmatrix} 99.44 & 533.60 \end{bmatrix}, \quad \hat{K}_{1,5} = \begin{bmatrix} 102.48 & 550.38 \end{bmatrix}, \quad \hat{K}_{1,6} = \begin{bmatrix} 102.98 & 538.35 \end{bmatrix},$$
$$\hat{K}_{1,7} = \begin{bmatrix} 100.40 & 541.86 \end{bmatrix}, \quad \hat{K}_{1,8} = \begin{bmatrix} 98.61 & 531.05 \end{bmatrix}, \quad \hat{K}_{1,9} = \begin{bmatrix} 103.57 & 550.09 \end{bmatrix},$$
$$\hat{K}_{1,10} = \begin{bmatrix} 104.04 & 536.49 \end{bmatrix}, \quad \hat{K}_{1,11} = \begin{bmatrix} 100.49 & 547.46 \end{bmatrix}, \quad \hat{K}_{1,12} = \begin{bmatrix} 99.79 & 537.14 \end{bmatrix},$$
$$\hat{K}_{1,13} = \begin{bmatrix} 104.01 & 548.72 \end{bmatrix}, \quad \hat{K}_{1,14} = \begin{bmatrix} 104.29 & 535.83 \end{bmatrix}, \quad \hat{K}_{1,15} = \begin{bmatrix} 99.43 & 547.46 \end{bmatrix},$$
$$\hat{K}_{1,16} = \begin{bmatrix} 99.24 & 536.97 \end{bmatrix}.$$

At iteration $k = 2$, the matrices $\hat{A}_{k-1,i}$ and $\hat{B}_{k-1,i}$ are obtained as follows:

$$\hat{A}_{1,1} = 11, \quad \hat{A}_{1,2} = 1, \quad \hat{B}_{1,1} = 0.08, \quad \hat{B}_{1,2} = 0.06.$$

and the controller gains $\hat{K}_{k,i}$ are:

$$\hat{K}_{2,1} = -1611.80, \quad \hat{K}_{2,2} = -1465.50$$

Appendix C. Average computation time

The following table shows the average computation time when two different approaches are applied to randomly generated mth-order systems, where $m = [2, 3, .., 7]$. The compared approaches are: the pole clustering approach introduced in this paper; and the traditional pole placement approach (see, e.g., Nguang and Shi (2006)). For each order m, 100 systems are generated and controlled using both approaches. Table C1 provides the average computation times in seconds Table C1 provides the average computation times in seconds obtained using MATLAB on a 3.60 GHz Intel(R) i7-9700K CPU computer. As we can see from the table, traditional pole placement performs faster than the approach proposed in this paper. However, the computational burden is still manageable in a reasonable time, with the main advantage that the pole clustering approach allows tailoring more specific performances associated to individual locations of the closed-loop poles.

Table C1. Average computation time (unit: seconds)

Pole clustering	$m = 2$	$m = 3$	$m = 4$	$m = 5$	$m = 6$	$m = 7$
	0.1227	0.1838	0.2526	0.3032	0.3723	0.4461
Pole placement	$m = 2$	$m = 3$	$m = 4$	$m = 5$	$m = 6$	$m = 7$
	0.0556	0.0590	0.0596	0.0629	0.0635	0.0652